DOI: 10.1021/ic9024537

Inorganic Chemistry
Article

Computational Exploration of the Mechanism of Alcohol Oxidation by Dioxygen Activated with Biquinolyl-Containing Cu Complexes

Pavel M. Polestshuk and Tatiana V. Magdesieva*

Dept. of Chemistry, M.V. Lomonosov Moscow State University, Leninskie Gory, 1/3 Moscow 119991, Russia

Received December 10, 2009

The mechanism of benzyl alcohol oxidation with dioxygen activated by Cu complexes with biquinolyl (biQ)-containing ligands was investigated using theoretical DFT calculations to identify the active species and to reveal similarities with naturally occurring oxidations performed by Cu-containing enzymes. The detailed potential energy profiles for two possible reaction paths with the α-H atom abstraction key step (*via* direct benzaldehyde formation and *via* hydroxylation of benzyl alcohol followed by the expulsion of a water molecule) were calculated for the both triplet and singlet states of a Cu(II)-superoxo complex and a Cu(III)-oxo complex. The DFT estimated activation barrier for the α-H-atom abstraction (which is involved in the both pathways) from a molecule of benzyl alcohol by the triplet biquinolyl-containing Cu(II)-superoxo complex is 16.4 kcal/mol. This value is reasonable for an enzymatic C−H bond activation and is very close to that calculated for benzylic C−H bond activation in dopamine and formylglycine. Thus, both reaction pathways are reasonable, and the existence of the parallel pathways cannot be ruled out. However, the first path (*via* direct benzaldehyde formation) is less complicated and the entropy factor should facilitate this route. (biQ)Cu(III)-oxo species formed in the catalytic cycle can also be involved in the further catalytic oxidation of the benzyl alcohol. DFT exploration performed for the triplet and singlet (biQ)Cu(III)-oxo complexes revealed that this process is barrierless and much more exothermic and, consequently, might be rather fast. It also includes the α-H-atom abstraction step and results in the formation of benzaldehyde. Thus, the primary catalytic cycle in which the Cu-superoxo complex performs the process can be coupled with the second cycle which is governed by the Cu-oxo complex formed in the first cycle.

I. Introduction

Oxygen activation occurs at a wide variety of metal-enzyme active sites.[1−6] Among these types of enzymes, Cu proteins play an important role.[6−14] They bind or activate dioxygen and perform a variety of critical biological functions. Depending on the function performed, Cu active sites have a different coordination environment and oxidation state; one or several copper centers can be involved in the catalytic process. Biomimetic copper chemistry provides a route for better understanding of the natural catalytic processes, contributing to the understanding of the structure of the active sites and the nature of the key intermediates in enzyme catalyzed processes.

Recently,[15,16] we developed an electrochemical approach (using a sacrificial Cu anode) to a new electroactive catalytic system based on polyamic acids (PA) with biquinolyl (biQ) fragments in the polymer backbone capable of coordination to Cu(I) ions (Scheme 1). Such ligands are able to stabilize reduced Cu(I) complexes without the often encountered

*Author to whom correspondence should be addressed. E-mail: tvm@org.chem.msu.ru.

(1) *Bioinorganic Chemistry: Inorganic Elements in the Chemistry of Life*; Kaim, W.; Schwederski, B., Eds.; Wiley: England, 1994; p 33.
(2) Halcrow, M.; Phillips, S.; Knowles, P. In *Subcellular Biochemistry, Vol. 35: Enzyme-Catalyzed Electron and Radical Transfer*; Holzenburg, A., Scrutton, N. S., Eds.; Plenum: New York, 2000; p 183.
(3) Holm, R. H.; Kennepohl, P.; Solomon, E. I. *Chem. Rev.* **1996**, *96*, 2239–2314.
(4) Kim, E.; Chufán, E. E.; Kamaraj, K.; Karlin, K. D. *Chem. Rev.* **2004**, *104*, 1077–1134.
(5) Collman, J. P.; Boulatov, R.; Sunderland, C. J.; Fu, L. *Chem. Rev.* **2004**, *104*, 561–588.
(6) Stubbe, J.; Van der Donk, W. *Chem. Rev.* **1998**, *98*, 705–762.
(7) Klinman, J. P. *Chem. Rev.* **1996**, *96*, 2541–2562.
(8) Whittaker, J. W. *Chem. Rev.* **2003**, *103*, 2347–2364.
(9) Fontecave, M.; Pierre, J.-L. *Coord. Chem. Rev.* **1998**, *170*, 125–140.
(10) Itoh, S. *Curr. Opin. Chem. Biol.* **2006**, *10*, 115–122.
(11) Lewis, E. A.; Tolman, W. B. *Chem. Rev.* **2004**, *104*, 1047–1076.
(12) Mirica, M. L.; Ottenwaelder, X.; Stack, T. D. P. *Chem. Rev.* **2004**, *104*, 1013–1046.
(13) Aboelella, N. W.; Kryatov, S. V.; Gherman, B. F.; Brennessel, W. W.; Young, V. G.; Sarangi, J. R.; Rybak-Akimova, E. V.; Hodgson, K. O.; Hedman, B.; Solomon, E. I.; Cramer, C. J.; Tolman, W. B. *J. Am. Chem. Soc.* **2004**, *126*, 16896–16911.
(14) Shearer, J.; Zhang, C. X.; Zakharov, L. N.; Rheingold, A. L.; Karlin, K. D. *J. Am. Chem. Soc.* **2005**, *127*, 5469–5483.
(15) Magdesieva, T. V.; Dolganov, A. V.; Yakimansky, A. V.; Goikhman, M. Ya.; Podeshvo, I. V.; Kudryavtsev, V. V. *Electrochim. Acta* **2008**, *53*, 3960–3972.
(16) Magdesieva, T. V.; Dolganov, A. V.; Yakimansky, A. V.; Goikhman, M. Ya.; Podeshvo, I. V.; Kudryavtsev, V. V. *Russ. J. Electrochem.* **2007**, *43*, 1133–1143.

Published on Web 02/25/2010

Scheme 1

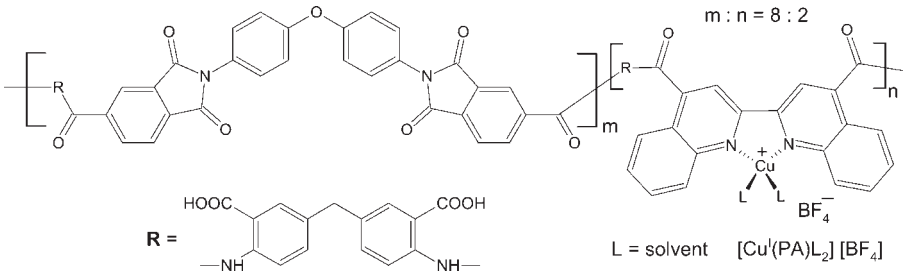

problem of disproportionation to Cu(0) and Cu(II). The obtained Cu(I) polymer complex showed high *oxidase* activity in the air-selective oxidation of aliphatic and aromatic alcohols,[15,16] as well as aliphatic amines,[17] to corresponding carbonyl derivatives, with concomitant reduction of molecular oxygen to water. The processes investigated are interesting as a possible new, efficient electrocatalytic route to synthetically useful organic compounds as well as in the mechanistic studies of copper catalyzed dioxygen activation in the oxidation of natural substrates.

The discussion of a possible reaction scheme[15,17] revealed that aerobic oxidation of aliphatic alcohols and amines follows a similar pathway. Both processes are catalyzed by the same type of Cu-containing catalytic species; both include the α-H-atom abstraction key step (it was confirmed by the presence of a small amount of a pinacol coupling product in the reaction mixture, as detected by GCMS) and have some other common features. Furthermore, we found some similarities with the natural catalytic cycle of alcohol oxidation with O_2 performed by *galactose oxidase* (*GO*); a protein comprised of a single polypeptide chain with one copper atom per active center.[8] One of the most important similarities is the formation of radical species responsible for the α-H-atom transfer key step. In addition, rough estimation of the redox powers of both systems revealed that they are comparable.[15,18] Though the coordination environments of our Cu complex and the active site of GO are quite different, the question arises of whether we can speak about *functional* modeling of natural enzymes.

In the present paper, we tried to computationally evaluate a possible reaction mechanism of alcohol oxidation catalyzed by a biquinolyl-containing Cu(I) complex. Reactions catalyzed by radical-dependent proteins are very diverse, and they play an important role in biosynthesis.[6] Referring to the natural enzymatic processes,[7] two possibilities were considered (Scheme 2).

In both reaction pathways, the substrate's C−H bond is cleaved by Cu/O_2 active species *via* an H-atom abstraction mechanism. In the first case, an aldehyde is formed directly, whereas the second approach includes α-hydroxylation of the starting alcohol followed by H_2O molecule release yielding an aldehyde. Path A resembles free radical catalysis by galactose oxidase (GO) observed in alcohol oxidation (Scheme 3).[7,8] Path B resembles that observed in the hydroxylation of β-phenylethylamine analogs, e.g., dopamine, performed by

Scheme 2

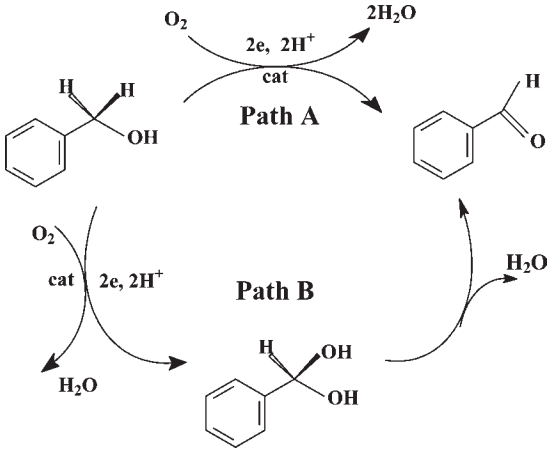

dopamine-β-monooxygenase (Dβ M) yielding norepinephrine formation (Scheme 3, path B-a). It is generally accepted that it involves a hydrogen atom abstraction step (as indicated by a large kinetic isotope effect of $k_H/k_D = 10.9$[19,20]).

Dβ M is similar in many aspects to peptidylglycine α-hydroxylating monooxygenase (PHM). PHM contains two uncoupled Cu centers (as in Dβ M) and requires dioxygen and an external reductant (ascorbic acid) for C−H bond activation, which is considered to proceed *via* the H-atom abstraction followed by the OH-group transfer (Scheme 3, path B-b).[21,22]

The nature of Cu/O_2 species involved in the catalytic processes performed by GO, Dβ M, and PHM has long been a subject of discussion.[7−14,23−25] Both experimental and computational evidence were presented, and it allowed the conclusion that two types of the most probable species, Cu(II)-superoxo and Cu(III)-oxo complexes, should be considered. These species are produced by dioxygen binding to a Cu center and are likely to be responsible for the C−H bond activation in the reactions performed by Dβ M[20,23,24,26] and PHM.[22,25] All of these reactions include the step of dioxygen reductive cleavage. The cleavage of the O−O bond in the

(17) Magdesieva, T. V.; Dolganov, A. V.; Yakimansky, A. V.; Goikhman, M. Ya.; Podeshvo, I. V. *Electrochim. Acta* **2009**, *54*, 1444–1451.
(18) Whittaker, M. M.; Whittaker, J. W. *J. Biol. Chem.* **1990**, *265*, 9610–9613.
(19) Miller, S. M.; Klinman, J. P. *Biochemistry* **1983**, *22*, 3091–3096.
(20) Kamachi, T.; Kihara, N.; Shiota, Y.; Yoshizawa, K. *Inorg. Chem.* **2005**, *44*, 4226–4236.
(21) Prigge, S. T.; Eipper, B. A.; Mains, R. E.; Amzel, L. M. *Science* **2004**, *304*, 864–867.
(22) Chen, P.; Solomon, E. I. *J. Am. Chem. Soc.* **2004**, *126*, 4991–5000.
(23) Yoshizawa, K.; Kihara, N.; Kamachi, T.; Shiota, Y. *Inorg. Chem.* **2006**, *45*, 3034–3041.
(24) Tian, G.; Berry, J. A.; Klinman, J. P. *Biochemistry* **1994**, *33*, 226–234.
(25) Crespo, A.; Marti, M. A.; Roitberg, A. E.; Amzel, L. M.; Estrin, D. A. *J. Am. Chem. Soc.* **2006**, *128*, 12817–12828.
(26) Evans, J. P.; Ahn, K.; Klinman, J. P. *J. Biol. Chem.* **2003**, *278*, 49691–49698.

Scheme 3

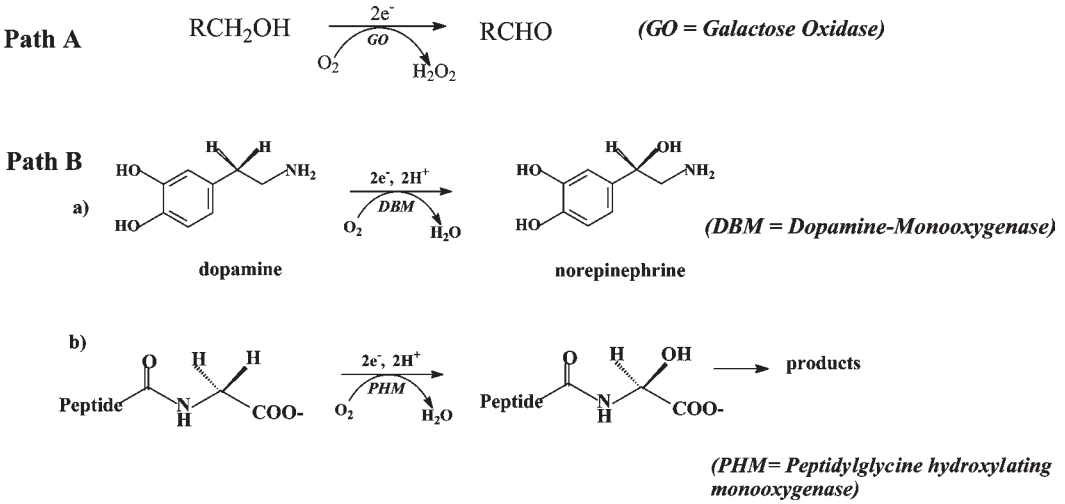

Cu(II)-hydroperoxo species prior to substrate activation is not feasible because of the high value of Cu(II)/Cu(III) redox potential.[27] It should be noted that, according to the recent data,[23] Cu(III)-oxo species can better mediate dopamine hydroxylation in the protein coordination environment of DβM than Cu(II)-superoxo species can. The calculated activation barrier for the hydrogen atom abstraction by Cu(II)-superoxo species is 23.1 kcal/mol, while that of the Cu(III)-oxo complex is 5.4 kcal/mol.[23]

In this study, two possible reaction pathways (Scheme 2) for benzyl alcohol oxidation yielding benzaldehyde were elucidated by DFT calculations in order to identify the reactive species involved, as well as to investigate the reaction thermodynamics and potential energy surfaces. The activation energies for the key steps were compared with those for enzymatic reactions. Two types of the active oxygen species were considered as the key reagents for α-H-atom abstraction at the benzylic position of the alcohol, Cu(II)-superoxo and Cu(III)-oxo complexes. Both triplet and singlet states of the reactive complexes were discussed. Cu-hydroperoxo species were not considered because their reactivity is not sufficient for C−H bond activation.[20,22]

II. Computational Details

All calculations were carried out with the PRIRODA quantum chemistry program.[28,29] The gradient-corrected exchange-correlation Perdew, Burke, and Ernzerhof (PBE) functional[30,31] was used for calculations. The efficient resolution of identity (RI) and parallel implementation of evaluating both Coulomb and exchange-correlation integrals with optimized fitting Gaussian basis sets in the PRIRODA code permits the performance of calculations of the molecular systems with a large number of basis functions.[28,29] A large integration grid (which comprises about 800 000 points over calculated molecules) with a 5×10^{-9} accuracy parameter of the adaptively generated grid was used. This parameter is responsible for the precision of the exchange-correlation energy per atom. The 10^{-7} threshold on the orbital gradients at the energy calculation stage and 10^{-5} threshold on the molecular gradient at the geometry optimization procedure were employed. For each singlet state computation, the triplet wave function as initial guess used. In all calculations, α and β electrons were treated independently; i.e., the spin-unrestricted formalism was chosen.

For all atoms except hydrogen, SBK effective core pseudopotentials were used.[32,33] The valence shells were described by basis sets with the following contraction schemes: [311/1] on H; [311/311/11] on C, N, and O; and [51111/51111/5111] on the Cu atoms. This basis set is denoted hereafter as SBK-TZ. In studying the **3-Min2a→3-MinP** and **1-Min2→1-MinP** transformations with four water molecules (see section III.2.c for details), the SBK-DZ basis set was used, which is described as [31] on H; [31/31/1] on C, N, O; and [51111/51111/5111] on Cu.

All geometries for the reaction species and transition states were completely optimized without any symmetry constraints. Systematic vibrational analysis was performed to confirm whether an optimized geometry corresponds to a transition state with only one imaginary frequency or to a local minimum without an imaginary frequency. Zero-point-vibrational-energy (ZPVE) corrections were taken into account in calculating the energetics of the reaction pathways. A rigid rotor and harmonic oscillator models were used for evaluation of the temperature (at 298 K) and entropy corrections for subsequent calculation of the Gibbs energies of the whole processes under discussion.

III. Results

In order to investigate possible reactive species and the subsequent reaction channels, the thermodynamics and potential energy surfaces were calculated using the PBE functional. The coordination environment of the reduced Cu(I) active site was modeled with the biQ ligand as part of the polymer backbone. According to our experimental data,[15] complexes with one biQ ligand in a Cu(I) coordination environment are very sensitive to dioxygen. In this interaction, dioxygen is first reduced to superoxide, concomitant with the oxidation of copper and formation of a (biQ)Cu(II)-superoxo complex. We started the computation with this type

(27) Miller, S. M.; Klinman, J. P. *Biochemistry* **1985**, *24*, 2114–2127.
(28) Laikov, D. N.; Ustynyuk, Y. A. *Rus. Chem. Bull.* **2005**, *54*, 820–826.
(29) Laikov, D. N. *Chem. Phys. Lett.* **1997**, *281*, 151–156.
(30) Perdew, J. P.; Burke, K.; Ernzerhof, M. *Phys. Rev. Lett.* **1996**, *77*, 3865–3868.
(31) Perdew, J. P.; Burke, K.; Ernzerhof, M. *Phys. Rev. Lett.* **1997**, *78*, 1396.
(32) Stevens, W. J.; Basch, H.; Krauss, M. *J. Chem. Phys.* **1984**, *81*, 6026–6033.
(33) Stevens, W. J.; Krauss, M.; Basch, H.; Jasien, P. G. *Can. J. Chem.* **1992**, *70*, 612–630.

Scheme 4

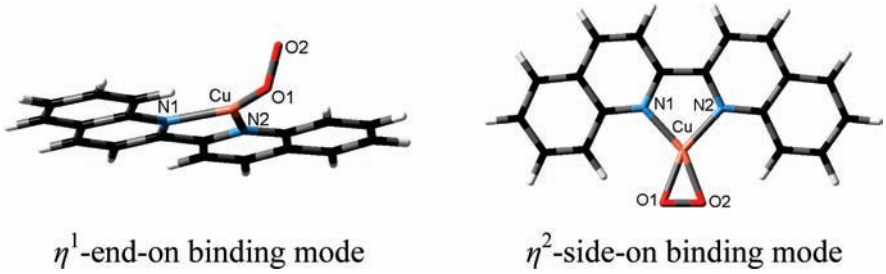

Table 1. Relative Values of Electronic (E_e^r, in kcal/mol) and ZPVE Corrected Energies (E_0^r, in kcal/mol), Hirschfield Charges (q), and Spin Populations (s, in parentheses)[a] on Selected Atoms for Calculated (biQ)Cu(II)-Superoxo Complexes in Triplet and Singlet Electronic States

species	E_e^r	E_0^r	Cu	O1	O2	d(Cu−O1), Å	d(Cu−N1), Å	d(O1−O2), Å	α(Cu−O1−O2), deg
3-η^2	0.0	0.0; (0.0,0.0,0.0)[d]	0.24(0.42)	−0.01(0.74)	−0.01(0.74)	2.001; (n/a,1.959, 1.952,1.920)[d]	1.980	1.305; (n/a,1.326, 1.311,1.295)[d]	71.0, 38.1[b]
1o-η^2	1.8	2.2; (5.5,3.6,3.6)[c]; (−4.3,-2.1, 7.3,12.4)[d]	0.26(0.00)	−0.06(0.00)	−0.06(0.00)	1.895; (1.967)[c]; (1.84,1.857, 1.813,1.854)[d]; (1.822,1.86)[f]	1.951	1.341; (1.276)[c]; (1.22,1.362, 1.356,1.325)[d]; (1.392,1.39)[f]	69.3, 41.4[b]
3-η^1	2.8	2.6; (0.0,0.0,0.0)[c]; (0.0)[g]	0.23(0.34)	0.00(0.67)	0.00(0.91)	1.848; (2.01)[g]	1.987	1.263; (1.23)[c]; (1.30)[g]	127.8; (110)[c]; (119.4)[g]
1c-η^2	4.6	5.4; (16.2,6.9,7.8)[c]	0.28	−0.09	−0.09	1.839	1.930	1.370	68.1, 43.7[b]
1o-η^1	8.0	7.9; (4.4)[g]	0.24(0.00)	−0.01(0.00)	−0.02(0.00)	1.834	1.979	1.269	126.9
1c-η^1	17.7	17.9; (23.0,14.8,32.4)[c]	0.24	−0.02	−0.08	1.809	1.960	1.282	125.6

[a] The spin populations are not presented for the cases for which the ground electronic state is described with the closed-shell wave function. [b] The value of the α(O1−Cu−O2) angle. [c] For Cu(II)-superoxo species of DβM (QM/MM), the first number corresponds to B3LYP/(TZV,D95), the second to BP86(6-311G*)//B3LYP/(TZV,D95), the third to PBE(6-311G*)//B3LYP/(TZV,D95), ref 20. [d] For the $Cu(O_2)$[HB(3-Ad-5-*i*Prpz)$_3$] side-on complex, the first value is experimentally measured, the second value is BP86/(6-311G*,6-31G*) calculated, the third value is B3LYP/(6-311G*,6-31G*) calculated, and the fourth value is B38HFP86/(6-311G*,6-31G*) calculated, ref 43. [e] X-ray data for PHM precatalytic enzyme complex.[21] [f] For the [$Cu(O_2)${β-diketiminate}] complex, the first number corresponds to X-ray data and the second to the BP86/(6-311+G*,6-31G*) calculated value, ref 35. [g] The (QM/MM) PBE/(DZV) calculated value for PHM complex, ref 25.

of a reactant complex for the calculation of both reaction pathways.

III.1. The Structure of the (biQ)Cu(II)-Superoxo Complex. The ground electronic state of the molecular dioxygen is the triplet ($X^3\Sigma_g^-$), and the lowest excited state (singlet, $A^1\Delta_g$) lies approximately 22 kcal/mol higher.[34] Consequently, there are two spin possibilities (the triplet and singlet electronic states) for the formation of the (biQ)Cu(II)-superoxo complex from the singlet [(biQ)Cu]$^+$ cation and molecular oxygen. In addition, the difference in the spin states, two types of coordination of molecular oxygen to the copper center, should be taken into account: the (η^1)-end-on and (η^2)-side-on fashions (Scheme 4). The PBE estimated relative energies of two types of superoxide complexes in (η^1)-end-on and (η^2)-side-on fashions for triplet (referred to here on as **3-η^1** and **3-η^2**, respectively) as well as closed-shell (**1c-η^1** and **1c-η^2**) and open-shell (**1o-η^1** and **1o-η^2**) singlet states are collected in Table 1. Hirschfield charges (q), spin populations (s) on selected atoms, as well as the key geometrical parameters for calculated (biQ)Cu(II)-superoxo complexes are also given in Table 1.

As follows from Table 1, the η^2-coordination type seems to be preferential as compared to the η^1 fashion. These data are in good agreement with the results of ref 35, in which the structures of 1:1 Cu/O_2 adducts were investigated. However, the mode of oxygen binding strongly depends on the nature of the ligands coordinated to the copper center.

The coordination of molecular oxygen to the Cu center also results in a 10-time decrease in the singlet/triplet gap of O_2. The O−O bond lengths in the first **3-η^2** and the second **1o-η^2** electronic states (Table 1) are not equal; the difference is about 0.04 Å. The reason for that, as well as for the stronger binding between Cu and O atoms (Cu−O bond is approximately 0.1 Å shorter in **1o-η^2** than in **3-η^2**), is the singlet state of dioxygen in the **1o-η^2** case. It should be noted that the energy of the open-shell singlet state **1o-η^2** is 3 kcal/mol lower than that for the closed-shell state **1c-η^2**. This is associated with the electronic structure of the dioxygen fragment within the complex, to which excited state the open-shell configuration is inherent.[36] The other type of singlet species **1c-η^1** with the open cycle has the lowest stability (E_0^r = 17.9 kcal/mol) among all investigated complexes. As for the charge distribution, the charges on the oxygen atoms are surprisingly small. This indicates the significant role of the nitrogen-containing ligand in the stabilization of the positively charged copper center. The spin density on the O atoms in the **3-η^2** is similar to that for the free dioxygen, with the values close to unity at both atoms.

The variety of literature data collected in Table 1 for comparison demonstrates the significant influence of the

(34) Herzberg, G. *Spectra of Diatomic Molecules*; Van Nostrand Reinhold: New York, 1950.

(35) Sarangi, R.; Aboelella, N.; Fujisawa, K.; Tolman, W. B.; Hedman, B.; Hodgson, K. O.; Solomon, E. I. *J. Am. Chem. Soc.* **2006**, *128*, 8286–8296.

(36) Schweitzer, C.; Schmidt, R. *Chem. Rev.* **2003**, *103*, 1685–1758.

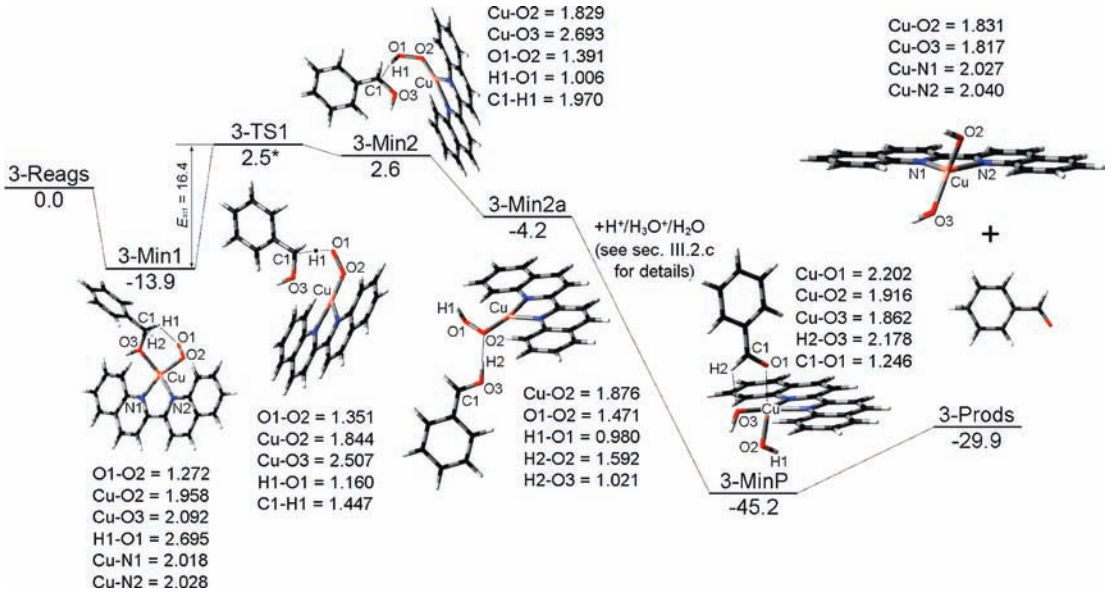

Figure 1. The potential energy profile (in kcal/mol) for benzyl alcohol oxidation with the triplet Cu-superoxo species (path A). All distances are given in Å. An asterisk stands for the case when ZPVE correction approximately equalizes the energies of **3-TS1** and **3-Min2** (see Table S2, Supporting Information).

choice of density functional as well as the nature of the ligands coordinated to the copper center on the relative energies of Cu(II)-superoxo species described. Analysis of the data in Table 1 reveals that the mode of oxygen binding to PHM or DβM (see refs 20, 21, and 25) differs from the other reported structures.[35] PHM and DβM are the macromolecules, whereas for small-molecule Cu−O_2 complexes the side-on binding mode is preferential in the majority of cases. As can be seen from Table 1 (see footnote f), our calculated geometric parameters d(Cu−O) = 1.895 Å and d(O−O) = 1.341 Å for the **1o-η^2** structure are qualitatively similar to the X-ray data obtained in ref 35 for [Cu(O_2){β-diketiminate}]: 1.822 Å (Cu−O) and 1.392 Å (O−O).

The two lowest electronic states, **3-η^2** and **1o-η^2**, were used as starting reagents in the subsequent computation. However, it should be noted that the small difference in energies of the first four electronic states does not allow for ruling out a possibility of the spin inversion in the reaction course. This is also facilitated by spin−orbit coupling due to the presence of the transition metal center.[37−42]

III.2. The Reactivity of the (biQ)Cu(II)-Superoxo Complex. As has been demonstrated in recent publications on the activity of Cu-containing enzymes DβM[20,23] and PHM,[22,25] the Cu(II)-superoxo complex is one of the most probable reactive species in oxidation processes. In both cases, the key step of the catalytic process is the α-H-atom abstraction from the substrate followed by O−OH bond cleavage and OH-group transfer.[20,22,23] This route corresponds to our path B, as has been already mentioned in the Introduction. Path A also includes the α-H-atom abstraction from the substrate, but it is not followed by the subsequent OH-group transfer and seems to be simpler. We will start the consideration of the reactivity of the (biQ)Cu(II)-superoxo complex with path A.

III.2.a. The Triplet State. Path A. Figure 1 shows a computed potential energy profile for path A; a direct alcohol oxidation by the triplet Cu(II)-superoxo species. Calculated atomic charges (q) and spin densities (s) for the reaction species are listed in Table S2 (Supporting Information). At the initial stage of the reaction, the substrate (benzyl alcohol) comes into contact with the Cu(II)-superoxo species to form a reactant complex (**3-Min1**) which has an energy 13.9 kcal/mol lower as compared to the separated reagents. A similar energy value (11.8 kcal/mol) was found in ref 20; however, it corresponds to an antiferromagnetically coupled singlet state. The optimized geometry of the reactant complex is presented in Figure 1. As can be seen from Figure 1, the coordination to the benzyl alcohol results in the opening of the Cu−O1−O2 cycle of the starting (biQ)Cu(II)O_2 (**3-η^2**). Hence, dioxygen is coordinated to a Cu center in the η^1-binding mode in **3-Min1**. The reason for this transformation is a small difference in the energies of **3-η^2** and **3-η^1** isomers (ΔE_0^r = 2.6 kcal/mol, Table 1). It should be noted that the $PhCH_2OH$ position is controlled by the interaction of the benzylic H1 atom and the O1 atom (d(H1−O1) = 2.695 Å). The calculated spin density on O1 is 0.86 (Table S2), indicating the presence of an unpaired electron on the O1 atom. [This is also related to (but to a lesser extent) the O2 Cu-ligating atom (s = 0.69, Table S2).] Therefore, this orientation is very favorable for a further H-atom abstraction step by the terminal O1-radical center.

The transition state **3-TS1** has O1−H1 and C1−H1 interatomic distances of 1.160 Å and 1.447 Å, respectively. These values are close to the distances obtained in ref 20 for the H-atom abstraction step in the DβM catalytic cycle (1.210 Å and 1.371 Å) in the antiferromagnetically coupled singlet state. The transition vector with the imaginary frequency of 1067i cm^{-1} (1816i cm^{-1} [20])

(37) Pyykkö, P. *Chem. Rev.* **1997**, *97*, 597–636.
(38) Fiedler, A.; Schroeder, D.; Shaik, S.; Schwarz, H. *J. Am. Chem. Soc.* **1994**, *116*, 10734–10741.
(39) Shaik, S.; Danovich, D.; Fiedler, A.; Schröder, D.; Schwarz, H. *Helv. Chim. Acta* **1995**, *78*, 1393–1407.
(40) Schröder, D.; Shaik, S.; Schwarz, H. *Acc. Chem. Res.* **2000**, *33*, 139–145.
(41) Shiota, Y.; Yoshizawa, K. *J. Chem. Phys.* **2003**, *118*, 5872–5879.
(42) Kondo, M.; Yoshizawa, K. *Chem. Phys. Lett.* **2003**, *372*, 519–523.

shows that this transition state is responsible for the H-atom abstraction step. The calculated activation energy is 16.4 kcal/mol. This value is reasonable for an enzymatic C−H bond activation and is very close to that calculated for benzylic C−H bond activation in dopamine (16.9 kcal/mol)[20] and formylglycine (∼14 kcal/mol)[22] and close to the experimental value of $\Delta H^{\neq}$ (∼13 kcal/mol) for the latter process. However, the calculated values obtained in ref 25 for PHM-catalyzed process are higher: 25 and 20 kcal/mol for the triplet and singlet states, respectively. In spite of this discrepancy, our data are in good agreement with the majority of other literature data, thus indicating that the activation barrier for H-atom abstraction by a Cu(II)-superoxo complex is not significantly influenced by the nature of the substituent at the benzylic carbon atom (CH_2NH_2 and OH). The calculated spin density distributed over all of the PhC$^{\bullet}$(H)OH moiety in **3-TS1** is 0.66. It indicates that the electron transfer from $PhCH_2OH$ to the [(biQ)Cu-OO] part of system is not complete.

After hydrogen transfer from the C1 to the O1 atom, the radical intermediate **3-Min2** was obtained, corresponding to the formation of the Cu(II)-hydroperoxo complex and the PhC$^{\bullet}$(H)OH radical coordinated to the Cu center with d(Cu−O3) = 2.693 Å. **3-Min2** has a relative energy of E_0^r = 2.6 kcal/mol. The calculated spin density on the C1 atom of **3-Min2** (0.38, Table S2, Supporting Information) is about one-third of the value corresponding to the PhC$^{\bullet}$(H)OH moiety (0.92), indicating electron delocalization over all carbon atoms of the phenyl group. It should be mentioned that the spin density on the O1 terminal atom of **3-Min2** is four times smaller compared to the s(O1) value for **3-Min1** due to O1−H1 bond formation (see Table S2).

It is interesting to note that the H1 atom transferred in the **3-Min1**→**3-TS1**→**3-Min2** step does not have significant spin density (Table S2, Supporting Information). Hence, H1 transfer is better described as a proton transfer. Therefore, this and the subsequent transformations dealing with the H-abstraction step would be better considered as a proton coupled electron transfer processes. This finding is also discussed in ref 22.

The recoordination of the PhC$^{\bullet}$(H)OH fragment in **3-Min2** results in the formation of **3-Min2a**, which is 6.8 kcal/mol more stable (Figure 1). A strong H2···O2 hydrogen bond (1.592 Å) is formed in **3-Min2a** instead of the H1···C1 contact (1.970 Å) observed in **3-Min2**. Apparently, this is the driving force for **3-Min2**→**3-Min2a** transformation. The calculated values of the charge (q) and spin density (s) on the PhC$^{\bullet}$(H)OH fragment in **3-Min2** (q = 0.19, s = 0.92) and **3-Min2a** (q = 0.33, s = 0.45) indicate the electron (and spin) density transfer from PhC$^{\bullet}$(H)OH to the Cu-hydroperoxo fragment. As a result, the electron structure of the PhC$^{\bullet}$(H)OH moiety converges to the $[PhCHOH]^+$ cation.

As will be demonstrated in section III.2.c, **3-Min2a** can be transformed with a low activation barrier to the preproduct **3-MinP** based on the (biQ)Cu(III)$(OH)_2$ complex in the presence of an external source of protons (it may be a molecule of the starting alcohol, the traces of water, or carboxy groups of the polymer backbone). It is a highly exothermic process with ΔE_0^r = −41 kcal/mol.

The energy of separated products ((biQ)Cu$(OH)_2$ and PhCHO) is 15 kcal/mol higher respective to **3-MinP**. However, it is strongly diminished when the presence of the solvent (CH_3CN or NMP) is considered. The molecules of the solvent can occupy free coordination places at the Cu center after benzaldehyde leaves the Cu coordination environment. Further electrochemical reduction of the (biQ)Cu$(OH)_2$ complex in the presence of protons finishes the catalytic cycle and restores the catalyst.

Path B. When evaluating the thermodynamics and energy barrier for H-atom abstraction by a side-on Cu(II)-superoxo triplet complex for the alternative reaction path B, we started with the same reactant complex. The relative energies, charges, and spin populations on the selected atoms of the calculated stationary points along the reaction coordinate are presented in Table S2 (Supporting Information). Five local minima were found for the reaction path B.

The initial steps of the process up to **3-Min2** are the same as in path A and have been discussed in detail in the previous section. The further reaction channel is different (Figure 2). The spin density values on O1, O2, and C1 atoms (see Table S2, Supporting Information) demonstrate that, in the next step, the O−O bond of **3-Min2** is homolytically cleaved and the O1H1 group is transferred to the C1 radical center of the substrate, forming a product complex *via* **3-TS2** with an imaginary vibrational frequency of 494i cm^{-1}. The **3-TS2** is only 2.5 kcal/mol higher in energy than **3-Min2**, thus indicating the small activation barrier of this process. This OH group transfer is a highly exothermic process with ΔE_r^0 = −38.8 kcal/mol (for the **3-Min2**→**3-Min3** transformation). This value is close to that obtained for DβM (−35.3 kcal/mol[21]) and substantially differs from the ΔG values calculated in ref 22 for formylglycine (−11 and −26 kcal/mol for singlet and triplet states, respectively). The optimized structure of **3-Min3** revealed a hydrogen bond formation between that of the diol's hydroxyl and that of the (biQ)Cu(III)-oxo complex (d(H1−O2) = 1.724 Å, Figure 2), which results in its additional stabilization. It should be noted that the spin population of the Cu atom in **3-Min3** (s = 0.66) is substantially higher than that in the Cu-superoxo or Cu-hydroperoxo complexes (see Table S2).

In this reaction step, the continuation of the process has alternatives (Figure 2). Molecular motion will facilitate diol's leaving the coordination sphere of the Cu ion followed by a H_2O release yielding benzaldehyde. One can expect that the thus formed Cu(III)-oxo complex can oxidize another molecule of benzyl alcohol and start the second catalytic cycle (see below). A fast intramolecular H-transfer from one of the hydroxyl groups to a free radical O2 center (s = 1.02) is an alternative reaction pathway. It is facilitated by the above-mentioned hydrogen bond in **3-Min3**, which is a precondition for diol's bonding with the Cu(III)-oxo complex, preventing its leaving into the bulk solution. The transition vector of **3-TS3** with the imaginary frequency of 898i cm^{-1}, which is something lower than that for **3-TS1** (1067i cm^{-1}), shows the C−H bond strength to exceed that for an O−H bond.

(43) Chen, P.; Root, D. E.; Campochiaro, C.; Fujisawa, K.; Solomon, E. I. *J. Am. Chem. Soc.* **2003**, *125*, 466–474.

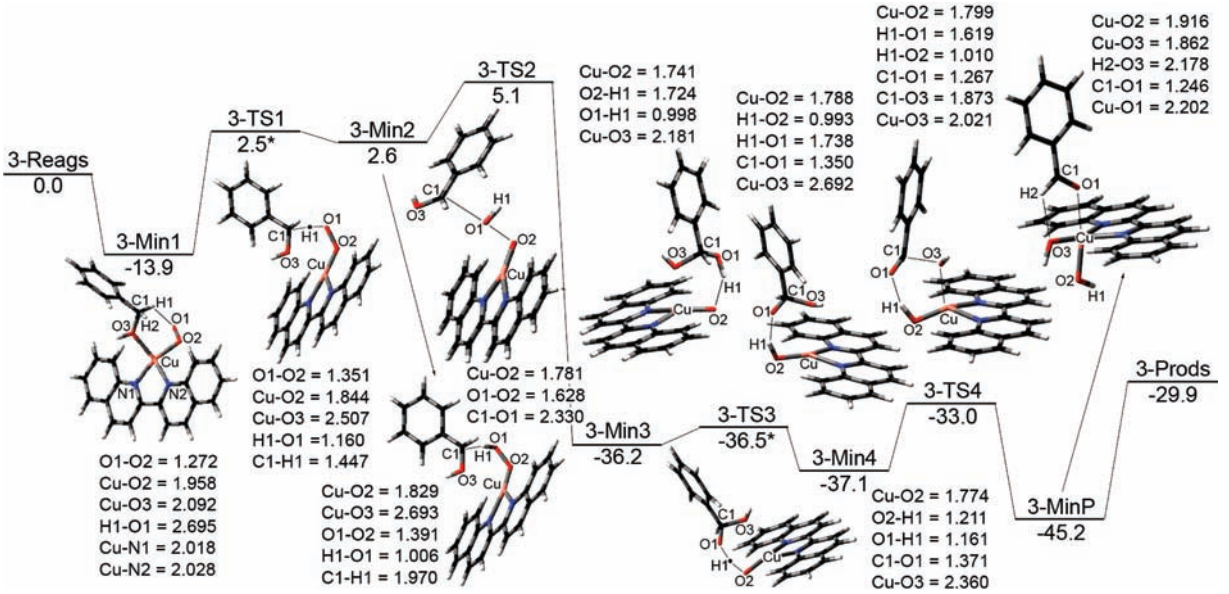

Figure 2. Potential energy profile (in kcal/mol) for benzyl alcohol oxidation with the triplet Cu-superoxo species (path B). All distances are given in Å. The asterisks stand for the cases when ZPVE correction approximately equalizes the energies of **3-TS1** and **3-Min2**, as well as **3-Min3** and **3-TS3** (see Table S2, Supporting Information).

The thus formed intermediate **3-Min4** is only about 1 kcal/mol more stable relative to **3-Min3**. However, OH-group transfer from the diol to the copper center *via* **3-TS4** with an activation energy of 4 kcal/mol yielding **3-MinP** results in a significant stabilization (~10 kcal/mol) of the reaction complex (Figure 2). The energy of **3-MinP** is 45.2 kcal/mol lower than the energy of the starting reagents. It depicts the (biQ)Cu(III)-dihydroxy complex coordinated with a molecule of benzaldehyde by means of a H2···O3 hydrogen bond (d = 2.178 Å) and Cu···O1 interaction (d = 2.202 Å). Thus, **3-MinP** is a final point in the proposed reaction scheme.

Comparing all activation barriers presented in Figure 2, one can conclude that a hydrogen atom abstraction, namely, the **3-Min1**→**3-TS1**→**3-Min2** process, is likely to be a rate-determining step of the overall reaction because it is the step with the maximal activation barrier. The same conclusion was drawn in some other papers based on the experimental data of a large kinetic isotope effect[18,19] as well as on the computation data.[20,22]

III.2.b. The Singlet State. Path A. As follows from Table 1, the open-shell singlet state of the (biQ)Cu(II)-superoxo complex **1o-η^2** is 2.2 kcal/mol less stable than **3-η^2**, but they both have a cyclic η^2 structure. The calculated potential energy profiles for the oxidation of benzyl alcohol with a singlet (biQ)Cu(II)-superoxo complex are given in Figures 3 and 4 for paths A and B. The calculated atomic charges (q) and spin densities (s) for the reaction species are listed in Table S4 (Supporting Information). In this section, the details of path A performed by the singlet species will be discussed (Figure 3). Comparing the reaction paths A obtained for the singlet and the triplet states (Figures 1 and 3) reveals several principal differences.

As follows from Figure 3, the coordination of benzyl alcohol to the Cu center does not result in the opening of the Cu−O1−O2 cycle as in the triplet case, and **1-Min1** still contains η^2-coordinated dioxygen. The relative energy E_0^{r1} of **1-Min1** for the singlet state (−12.6 kcal/mol) is close to the value obtained in ref 22 for the antiferromagnetically coupled singlet state (E_0^{r1} = −11.8 kcal/mol) and is not significantly different from the corresponding value for **3-Min1** (−13.9 kcal/mol, see Figure 2). [It should be noted that the starting energies of the triplet and singlet reagents are different (see Figures 1−4), according to the energies of the starting Cu-superoxo complexes used (see Table 1). Here, we introduce E_e^{r1} (E_0^{r1}) and E_e^{r3} (E_0^{r3}) values, which are calculated relative to **1-Reags** and **3-Reags**, respectively. The complete comparative analysis of the calculated stationary points with different multiplicities will be presented below in the Discussion section.]

The H-atom abstraction from the benzylic position occurs in the next step of the process. The relative energies (E_0^{r1} or E_0^{r3}) of **1-TS1**, as well as the calculated value of activation energy, 14.1 kcal/mol for the singlet state, are comparable to that obtained for the triplet complex. Consequently, the main conclusions drawn in the previous section for the **3-Min1**→**3-TS1**→**3-Min2** step of path A for the triplet species can also be extended for the same transformation performed in the singlet state. It should be noted that the comparison of $\Delta E_0^{\neq}$ = 14.1 kcal/mol obtained for the singlet state with the value of benzylic C−H bond activation in dopamine (16.9 kcal/mol)[20] is more correct, because these data also correspond to the antiferromagnetically coupled singlet state of the reactant.[20]

The changing of the spin state of Cu-superoxo species results in a 0.06 Å increase in the H1−O1 distance and in the diminution of the C1−H1 distance (for 0.09 Å) in **1-TS1**. In addition, the spin population values (s) of the O1 and O2 oxygen atoms in **1-TS1** (Table S4, Supporting Information) are substantially lower, as compared to **3-TS1** (Table S2, Supporting Information). The other geometric parameters for **TS1** in Figures 1 and 3, as well as the value of the imaginary frequency of the transition vector (1160i cm^{-1}), do not differ significantly.

The structure of **1-Min2** is generally similar to **3-Min2a** in the triplet path, except for one detail: in **1-Min2** the Cu

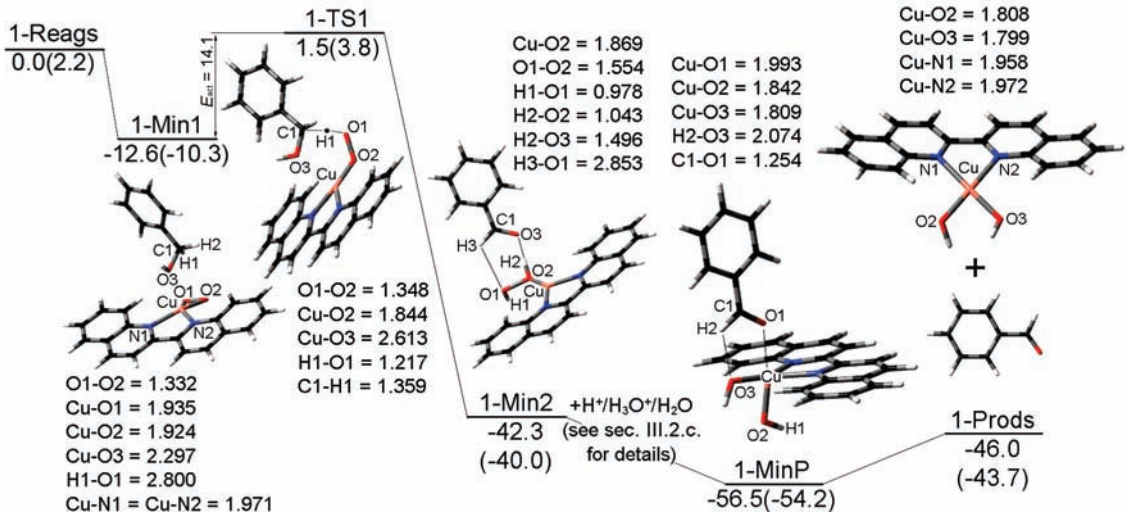

Figure 3. Potential energy profile (in kcal/mol) for benzyl alcohol oxidation with the singlet Cu(II)-superoxo species (path A). The specified energies correspond to $E_0^{\tau 1}$ and $E_0^{\tau 3}$ (in parentheses). All distances are given in Å.

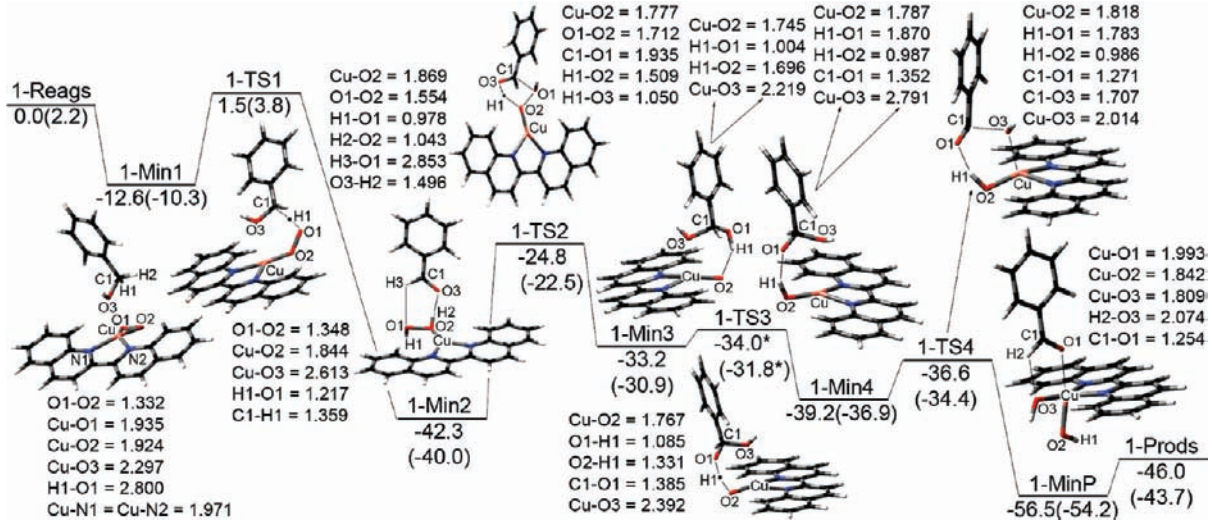

Figure 4. Potential energy profile (in kcal/mol) for benzyl alcohol oxidation with the singlet Cu(II)-superoxo species (path B). The specified energies correspond to $E_0^{\tau 1}$ and $E_0^{\tau 3}$ (in parentheses). All distances are given in Å. The asterisks stand for the cases when ZPVE correction approximately equalizes the energies of **1-Min3** and **1-TS3** (see Table S4, Supporting Information).

center is coordinated to the peroxide molecule (Figure 3), whereas in **3-Min2a** it is bound to the hydroperoxo fragment (Figure 1). This indicates that the H-atom transfer from the O3-hydroxy group to the O2-oxygen atom bound to the Cu center is a barrierless process in the singlet case. According to our computations, the ground electronic state of **1-Min2** system is of the closed-shell type (see Table S4, Supporting Information) and is 35.8 kcal/mol more stable than **3-Min2a**. The O1−O2 bond in the peroxide coordinated to the copper complex in **1-Min2** is substantially longer (d = 1.554 Å) as compared to the calculated value for a free H_2O_2 molecule (d = 1.475 Å). It should be noted that our attempts to localize the geometry of the triplet state of the same complex failed because of the spontaneous O1−O2 bond breakdown.

As was already mentioned in the discussion of the triplet state, the possibility of **1-Min2** transformation into preproduct **1-MinP** based on the (biQ)Cu(III)$(OH)_2$ complex will be considered in section III.2.c. Similar to the triplet case, it demands an external source of protons, but it is much less exothermic (ΔE_0^{τ} = −14 kcal/mol), as compared to the **3-Min2a**→**3-MinP** transformation (ΔE_0^{τ} = −41 kcal/mol). The consequent release of a benzaldehyde molecule leads to **1-Prods** (benzaldehyde + (biQ)Cu$(OH)_2$) and increases the energy for 10 kcal/mol (Figure 3).

Path B. Similarly to the triplet case, the beginning of the process (up to **1-Min2**) is the same for paths A and B in the singlet state (compare Figures 3 and 4). The calculated values of relative energies, atomic charges (q), and spin densities (s) for the reactive species of path B are listed in Table S4 (Supporting Information). The computations revealed that the continuation of the process provides the same final energy stabilization (**1-MinP** and **1-Prods**) as in the previous case of path A, but it needs passing of a rather high energy barrier between **1-Min2** and **1-Min3** which is equal to 17.5 kcal/mol and corresponds to the **1-TS2**.

A concerted transfer of the H atom and OH group of the peroxide fragment to the carbon atom through transition state **1-TS2** with an imaginary vibrational

frequency of 288i cm^{-1} leads to **1-Min3**. As has been already mentioned, the activation barrier of this process is the maximum ($E_0^{\neq}$ = 17.5 kcal/mol) among all other transformations in Figure 4. The lengths of H1−O2 (d = 1.509 Å), H1−O3 (d = 1.050 Å), C1−O1 (d = 1.935 Å), and O1−O2 (d = 1.712 Å) bonds in five-membered transition state **1-TS2** (Figure 4) match the conclusion above about the concerted character of this step. Surprisingly, the ground electronic state of **1-TS2**, which comprises many broken bonds, is described by the closed shell wave function, as it was in **1-Min2** (see Table S4, Supporting Information).

The $E_0^{\neq}$ activation value for the **1-Min2→1-TS2→1-Min3** transformation obtained in the present work significantly exceeds the value calculated in ref 20 for a similar step including a Cu-superoxo antiferromagnetically coupled singlet state species (**I-so→TS2-so→P-so**, $E_0^{\neq}$ = 9.7 kcal/mol). This difference is more likely attributed to additional energy necessary for H1 atom transfer from the O2 Cu-ligating atom to the O3 atom of the benzaldehyde fragment in the **1-Min2→1-TS2→1-Min3** transformation.

Though **1-Min3** is 9 kcal/mol less stable than **1-Min2**, the follow-up transformations **1-Min3→...→1-MinP**, including two negligible barriers (**1-TS3** and **1-TS4**), result in a significant energy stabilization: 14.2 kcal/mol respective to **1-Min2** and 23.3 kcal/mol respective to **1-Min3** (Figure 4). All structural modifications occurring in the **1-Min3→1-TS3→1-Min4** (ΔE_0^r = −6 kcal/mol) and **1-Min4→1-TS4→1-MinP** (ΔE_0^r = −17 kcal/mol) steps are similar to those discussed earlier for the triplet state species of path B.

The overall thermodynamics of both paths A and B are identical (**1-Reags** and **1-Prods** are the same); however, the reaction path B presented in Figure 4 is less probable as compared to path A (Figure 3) due to the significant activation barrier in **1-Min2→1-TS2→1-Min3** transformation. For convenience, the complete comparison of four possible routes (both singlet and triplet states for paths A and B) will be given in section IV (Discussion).

III.2.c. 3-Min2a→3-MinP and 1-Min2→1-MinP transformations of Path A. A more detailed consideration of the **3-Min2a→3-MinP** and **1-Min2→1-MinP** transformations which take place in the presence of water molecules (or other sources of protons) is presented below.

As was demonstrated earlier, **3-Min2**, formed after the H-atom abstraction from benzyl alcohol, either participates in **3-Min2→3-Min3** conversion (path B, see Figure 2) or transforms into **3-Min2a**, yielding preproduct **3-MinP** in the presence of a source of protons (path A, see Figure 1). In both cases, the O−O bond is cleaved, yielding a significant energy stabilization (approximately 40 kcal/mol, Figures 1 and 2). In the case of **1-Min2**, the energy stabilization is smaller (14 kcal/mol, Figures 3 and 4).

The O−O bond cleavage in these transformations is accompanied by the protonation of the terminal oxygen atom (O1). Both processes occur simultaneously and are interrelated. That means that one of the processes initiates the other, and coupling of the two processes takes place. For example, after the O−O bond elongation the O1 atom becomes more prone to the capture of an H atom or a proton. On the other hand, the approach of a proton or an H-donating molecule to the O1 atom results in O−O bond breaking. For further clarification, both processes will be modeled by two independent relaxed scans along the O1−O2 and H1−O1 coordinates. This allows us to evaluate the energetics of these transformations. [All computations in this section were performed using the SBK-DZ basis set. Hence, some results obtained here might slightly differ (1−2 kcal/mol) from the data presented above for the SBK-TZ basis set.]

To our knowledge, the protonation of Cu(II)-hydroperoxo complexes has not been investigated in detail in the literature. As was mentioned in a recent paper,[25] the addition of a proton to the $[Cu^{II}-OOH]^+$ system results in a spontaneous barrierless O−O bond cleavage forming $[Cu^{II}O\cdots HOH]^{+2}$. In addition, it was shown[22,44] that a H-atom abstraction from formylglycine with the terminal O-atom initiates a homolytic cleavage of the O−O bond (with an activation barrier of 37 kcal/mol), yielding a Cu(III)-oxo complex and a water molecule. If the Cu-ligating O atom participates in an H-abstraction step, the O−O bond is also cleaved.[22]

Homolytic cleavage of the O−O bond in Cu-hydroperoxo complexes in the absence of the external source of protons or H-atoms yielding Cu(III)-oxo species and a $HO^{\bullet}$ radical was studied more extensively. It is an endothermic process with ΔG ~47 kcal/mol (ΔE ~59 kcal/mol[22] and ~75 kcal/mol[44]) for the singlet state and ΔG ~32 kcal/mol[22] (ΔE ~44 kcal/mol[22]) for the triplet state. Thus, we can conclude that this process is very unfavorable thermodynamically. However, it should be mentioned that the data presented above were obtained for media of low polarity (ε = 5).

According to our calculations, the addition of a proton to the terminal O1 atom in **3-Min2** results in a reverse H-atom transfer to the radical α-carbon center and the formation of $[PhCH_2OH\cdots HOOCu(biQ)]^{+2}$. The reason is the small energy barrier for this transformation (see Figure 1). However, the above described possibility of an easy conversion of **3-Min2** to a more stable isomer **3-Min2a** (the difference in E_0^r values is −6.8 kcal/mol, Figure 1), accompanied by a significant decrease in spin density in the "PhCHOH" fragment (0.45 for **3-Min2a** vs 0.92 for **3-Min2**), allows an avoidance of this reverse H-atom transfer. Furthermore, the addition of either a bare proton or a hydroxonium ion (H_3O^+) to the O1 atom in **3-Min2a** induces a spontaneous O1−O2 bond cleavage, as was observed in ref 25. Similarly, the protonation of the ligating O2 atom also causes homolytic O−O bond cleavage. This consideration is also applicable to **1-Min2**, in which the O1−O2 bond is 0.083 Å longer than that in **3-Min2a** (Figures 1 and 3) and, consequently, more prone to the breakdown.

In the previous consideration, we used H^+ or H_3O^+ as a proton donor. It should be mentioned that this is not absolutely correct due to their high reactivity and small concentration in the reaction mixture. Therefore, we investigated a possibility for the protonation of **3-Min2a** and **1-Min2** with water. For modeling of the process, four water molecules were used. At least two of them are necessary to fill free coordination places in the copper coordination environment.

(44) Chen, P.; Fujisawa, K.; Solomon, E. I. *J. Am. Chem. Soc.* **2000**, *122*, 10177–10193.

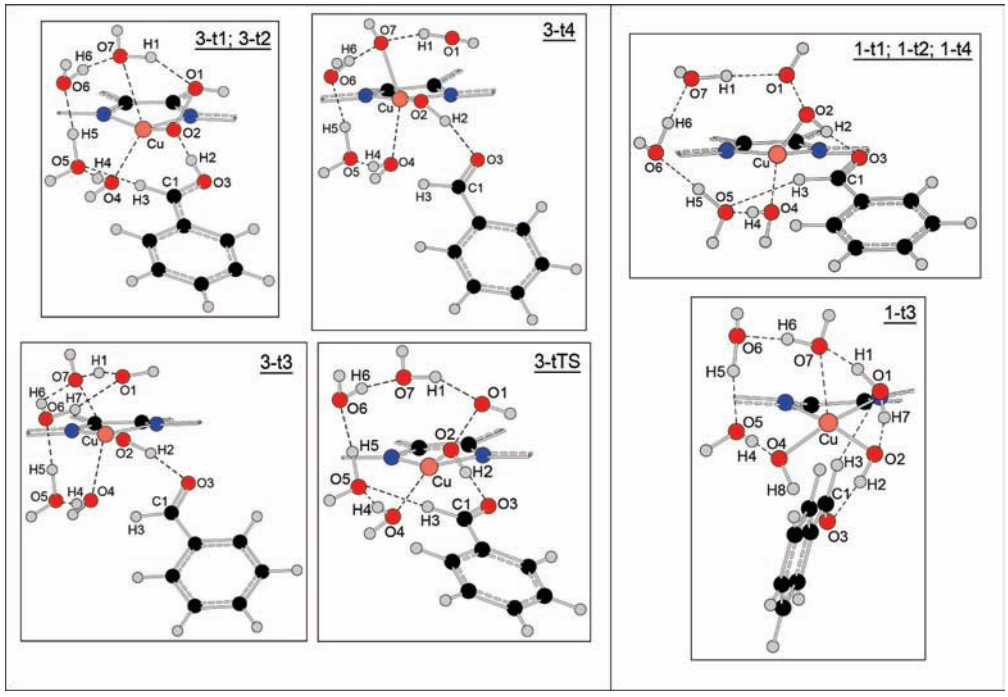

Figure 5. Geometries of the most relevant species denoted by bold points in Figure 6. A substantial part of the biQ fragment is omitted for the clarity.

The hydratation of **3-Min2a** and **1-Min2** with four water molecules (a tetramer $(H_2O)_4$) results in the formation of products **3-t1** (ΔE_0 = −24.6 kcal/mol) and **1-t1** (ΔE_0 = −17.8 kcal/mol), respectively (see Figure 5). In these products, the newly formed hydrogen bonds (H1···O1, H2···O2, and H3···O5 for **3-t1**, see Figure 5 and Table S6 (Supporting Information), and H1···O1, H2···O3, and H3···O5 for **1-t1**, see Figure 5 and Table S6) are present, as well as several hydrogen bonds of the $(H_2O)_4$ tetramer being partially reserved. These are the bonds H4···O5, H5···O6, and H6···O7 in **3-t1** and in **1-t1** (see Figure 5 and Table S6). The coordination of a water molecule $H_2O(7)$ to the Cu center also contributes to the additional stabilization of **3-t1** as compared to **1-t1** (see Figure 5 and Table S6).

Now let us consider the scan curves along the H1−O1 and O1−O2 coordinates (Figure 6). The geometries of the systems denoted by the bold points in Figure 6 are presented in Figure 5, and the main bond lengths are given in Table S6 (Supporting Information). As follows from Figure 6a, the scanning along the H1−O1 coordinate, which started from the singlet **1-t1**, leads to the O−O bond breaking at the **1-t2** point with d(H1−O1) = 1.290 Å and d(O1−O2) = 1.830 Å. The energy of **1-t2** is about 5.1 kcal/mol higher as compared to **1-t1**. We failed to detect any stationary point in the vicinity of **1-t2** in the potential energy surface. Hence, the **1-t1**→**1-t3** conversion has no transition state, and we can conclude that the **1-t2** point lies simply on the intersection of two potential energy surfaces. The same picture was observed for the O−O scanning of the singlet state (Figure 6b), but for the **1-t4** point, E_e^r is equal to 16.8 kcal/mol (or 2.3 kcal/mol relatively to **1-t1**) and corresponds to the following bond lengths: d(H1−O1) = 1.595 Å and d(O1−O2) = 1.933 Å (Table S6). On the basis of these data one can conclude that the preferential path of **1-t1**→**1-t3** conversion is **1-t1**→**1-t4**→**1-t3**. These consecutive steps include a primary O−O bond cleavage, which initiates a cascade migration of the protons (with subsequent electron transfers), H1→O1, H6→O7, H5→O6, and H4→O5, as shown in the Scheme 5 (see Figure 5 and Table S6 also). These results are supported by recent works which state that water-mediated hydrogen bonds are effective coupling elements for electron transfer.[45,46]

The curve obtained in the relaxed scan along the H1−O1 coordinate for the triplet state is disrupted in the vicinity of points **3-t2** (with d(H1−O1) = 1.427 Å) and **3-t3** (with d(H1−O1) = 1.336 Å, Figure 6a). As a result, two disjointed curves are formed: (1) the **3-t1**→**3-t2** curve, corresponding to a continuous increase in energy (Figure 6a) and (2) the **3-t3**→**3-t4** curve, reflecting a monotonous decrease in energy to the minimum **3-t4** (4 kcal/mol, Figure 6a). These fragments of the potential energy surface are interconnected *via* variation of the other independent coordinate, the O1−O2 bond length. The dotted arrow in Figure 6a shows that **3-t2**→**3-t3** switching between two curves is performed through the O1−O2 bond breaking, as confirmed by the values of d(O1−O2) for **3-t2** (1.459 Å) and **3-t3** (2.179 Å) (Table S6, Supporting Information).

The **3-tTS** transition state is observed in the scan curve along the O1−O2 coordinate for the triplet state. It is characterized by energies of E_e^r = 45.2 and E_0^r = 42.0 kcal/mol, corresponding to the bond distances d(O1−O2) = 1.596 Å and d(H1−O1) = 1.771 Å (Figure 6b, Table S6, Supporting Information) and an imaginary frequency of 786.0i cm^{-1} corresponding to O1−O2 bond cleavage. It means that O1−O2 bond breaking in **3-t1** demands overcoming of a very small barrier (1.8 kcal/mol

(45) Ponce, A.; Gray, H. B.; Winkler, J. R. *J. Am. Chem. Soc.* **2000**, *122*, 8187–8191.
(46) Tezcan, F. A.; Crane, B. R.; Winkler, J. R.; Gray, H. B. *Proc. Natl. Acad. Sci. U.S.A.* **2001**, *98*, 5002–5006.

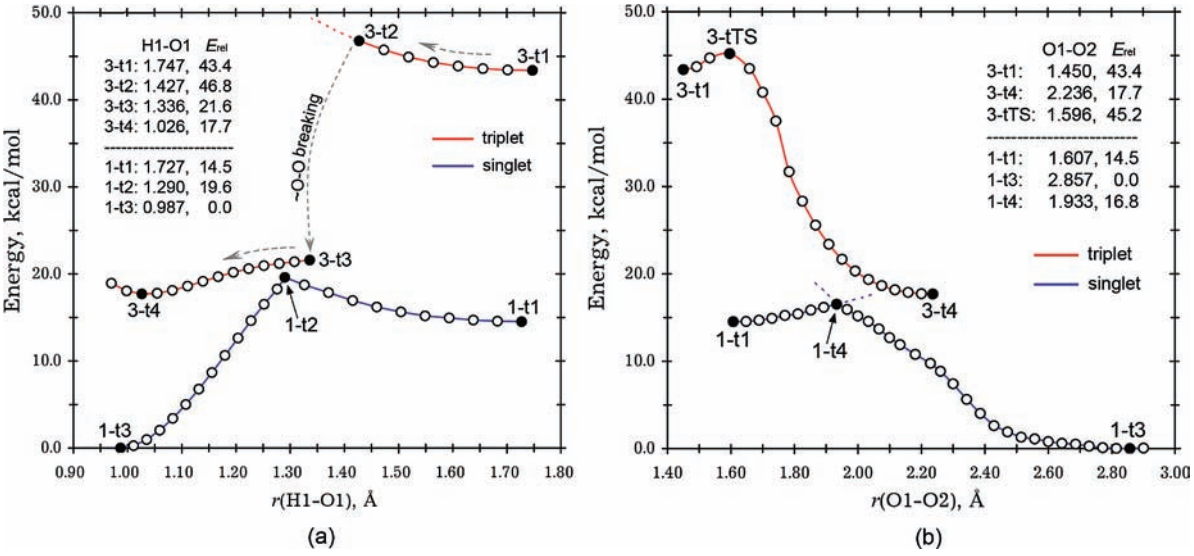

Figure 6. Two independent relaxed scans of **3-t1** and **1-t1**. Plot (a) depicts the paths along the H1−O2 mode. Plot (b) shows a relaxed energy scan along the O1−O2 mode. All distances are in Å; relative electronic energies are in kcal/mol and calculated relatively to **1-t3**.

Scheme 5

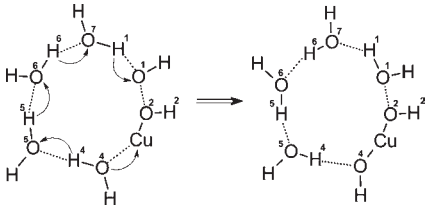

or even only 0.1 kcal/mol taking into account ZPVE correction). The energy of the **3-t2** point in the **3-t1→3-t2** curve is 3.4 kcal/mol higher than **3-t1**; consequently, **3-t2** has enough energy to overcome the barrier corresponding to **3-tTS**. This makes **3-t2→3-t3** conversion discussed above (see Figure 6a) quite reasonable.

A low activation barrier is attributed not only to the presence of water molecules but also to the H2 atom transfer from the PhCHOH fragment to the Cu-ligating O2 atom in the course of **3-t1→3-tTS→3-t4** conversion. It follows from the comparison of the H2−O2 bond distances: d(H2−O2) = 1.474 Å in **3-t1** and d(H2−O2) = 1.040 Å in **3-tTS** (Figure 5, Table S6, Supporting Information). The formation of the H2−O2 bond weakens the O1−O2 bond and lowers the activation barrier. This conclusion is also correct for the singlet state in which the H2−O2 bond is already present at the **1-t1** point (Figure 5, Table S6).

A small activation barrier corresponding to **3-tTS** indicates that the initial step in **3-t1→3-t4** conversion is O−O bond cleavage, which induces barrierless H1-abstraction from the water molecule $H_2O(7)$ (see Figure 5 and Table S6 (Supporting Information), and this also concerns the singlet state). In the triplet case, the cascade proton transfer is not observed, probably due to the presence of a short Cu···O7 contact in all triplet species (Table S6), which stabilizes the fragment formed after the H1−O7 bond cleavage *via* its coordination to the Cu center followed by Cu−O7 bond formation (d = 1.983 Å for **3-t4**).

To summarize, we can conclude that the protonation of the $[PhCHOH\cdots HOOCu(biQ)]^+$ complex (**3-Min2a** or **1-Min2**) to the O1 atom is possible not only with highly active species such as H^+ or H_3O^+ but with water molecules as well. Albeit, in the latter case, **3-Min2a→3-MinP** and **1-Min2→1-MinP** transformations are initiated by the O−O bond cleavage, with the activation barriers of these processes ≤ 2−3 kcal/mol. In the absence of the PhCHOH fragment, an active Cu(III)-oxo system is probably formed, which can further participate in the oxidation of benzyl alcohol (see below) or be stabilized by H-atom abstraction, e.g., from the water molecule. This conclusion is in good agreement with the literature data. For example, the formation of Cu(III)-oxo species after protonation of the hydroperoxo complex is, according to ref 25, one of the key processes occurring in hydroxylation catalyzed by peptidylglycine α-hydroxylating monooxygenase (PHM). The detailed experimental investigation of the hydroperoxo system (biQ)CuOOH performed in ref 17 also revealed that its reactivity is significantly increased in the presence of water molecules. In our opinion, this could be attributed to the formation of the active Cu(III)-oxo species.

Because the active sites of the enzymes are highly solvent accessible,[47,48] the hydroperoxo complex formed in the first step of hydroxylation can either be transformed to the by Cu(II)(OH) complex or it can participate in further reactions as the Cu(III)-oxo complex. This explains the absence of the hydroperoxo complex in the reactions of enzymatic hydroxylation.[7]

III.3. The Reactivity of the (biQ)Cu(III)-Oxo Complex. All reaction paths considered above (see Figures 1−4) include the formation of the (biQ)Cu(III)-oxo complex. Thus, the intermediate species which participate in **3-Min2a→3-MinP** and **1-Min2→1-MinP** transformations in path A (Figure 5) may be considered as a potential sources of the (biQ)Cu(III)-oxo complex in the moment of O1−O2 bond breaking. **1-Min3** and **3-Min3** in

(47) Prigge, S. T.; Kolhekar, A. S.; Eipper, B. A.; Mains, R. E.; Amzel, L. M. *Science* **1997**, *278*, 1300–1305.
(48) Prigge, S. T.; Kolhekar, A. S.; Eipper, B. A.; Mains, R. E.; Amzel, L. M. *Nat. Struct. Biol.* **1999**, *6*, 976–983.

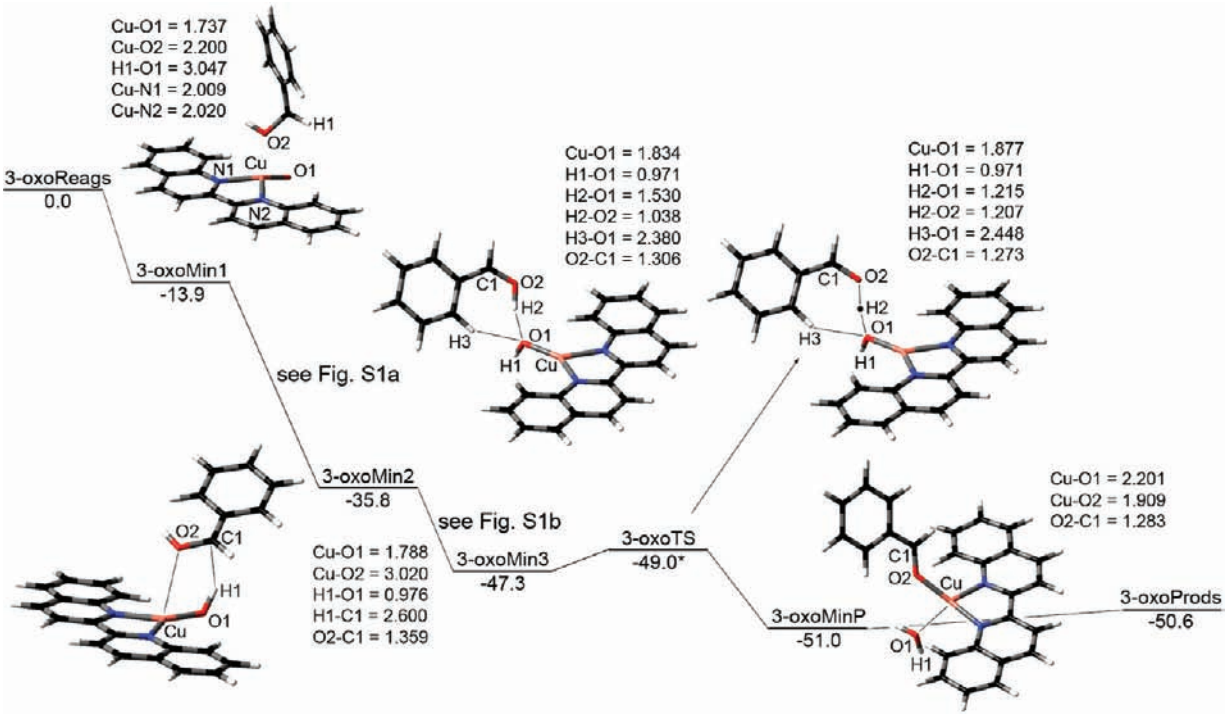

Figure 7. Potential energy profile (in kcal/mol) for benzyl alcohol oxidation with Cu(III)-oxo species (triplet electronic state). All distances are given in Å. The asterisk stands for the case when ZPVE correction approximately equalizes the energies of **3-oxoMin3** and **3-oxoTS** (see Table S8, Supporting Information).

path B (for the singlet and triplet states) also include this complex. According to the literature data,[20,23] the ability of the Cu(III)-oxo complex to abstract the H atom at a benzylic position of a dopamine molecule was estimated to be even higher than that for Cu(II)-superoxo species. This fact stimulated us to perform a DFT calculation of the catalytic cycle of aerobic oxidation of the benzyl alcohol with this type of active oxygen species (which can be formed in the course of the primary reaction of an initially formed Cu(II)-superoxo complex with benzyl alcohol). The oxidation of $PhCH_2OH$ with the triplet (biQ)Cu(III)-oxo complex will be considered first.

III.3.a. The Triplet State. The complete energy profile for the oxidation path is given in Figure 7. The relative energies, calculated atomic charges (q), and spin densities (s) for the reaction species are presented in Table S8 (Supporting Information). The whole process includes four minima and only one transition state. This indicates that all steps but one are barrierless. An alcohol oxidation mediated with the Cu(III)-oxo species starts with the formation of a reactant complex **3-oxoMin1**, which is 13.9 kcal/mol more stable than the starting **3-oxoReags**. The formation energy for the same adduct obtained in ref 20 is lower (8.3 kcal/mol). If the formation of **3-oxoMin1** is considered as the replacement of a molecule of a solvent (e.g., CH_3CN) by $PhCH_2OH$, which comes into contact with the Cu center, it gives a small energy loss. The PBE/SBK-TZ estimated formation energies for two systems, [(biQ)Cu=O·(CH_3CN) and $PhCH_2OH$] and [(biQ)Cu=O·($PhCH_2OH$) and CH_3CN], are almost the same: the former is only 2.4 kcal/mol more stable. This difference seems not to be significant because the coordination of $PhCH_2OH$ to a Cu center starts a downhill barrierless **3-oxoMin1**→**3-oxoMin2** process toward product formation.

The first step of the mechanism under consideration is an H abstraction with the O1 atom bearing an odd electron (s(O1) = 1.16, Table S8, Supporting Information), as in all previous schemes. According to our computation data, **3-oxoMin1**→**3-oxoMin2** transformation is barrierless (Figure 7), and it significantly lowers the total energy (~22 kcal/mol). In the papers cited above discussing the dopamine[20,23] and peptidylglycine[25] hydroxylation, the similar transformations yet have a small activation barrier: $E_0^{\neq}$ = 3.8,[20] 5.4,[23] and 4.1[25] kcal/mol. The stabilization energy in the similar transformations of dopamine are almost identical, regardless of whether surrounding amino acid residues are considered (14.2[23] kcal/mol) or not (16.6[20] kcal/mol). The value obtained for peptidylglycine is lower[25] (7.1 kcal/mol). Thus, the stabilization energies observed in the literature cited above[20,23,25] are smaller than in our case (see Figure 7).

The results of H1 atom abstraction scanning along the H1−O1 coordinate (see Figure S1a, Supporting Information) reveal a monotonously decreasing plot without any maximum, thus indicating the absence of any stationary points. It is interesting to note that the point corresponding to the H1−O1 distance of 1.189 Å (**3-oxoMid1**) is 10 kcal/mol lower in energy than **1-oxoMin1** and does not satisfy any transition state, contrary to **3-TS1** (Figure 1 and 2) with almost the same (H1−O1) distance (1.160 Å).

The following steps of benzyl alcohol oxidation with the triplet Cu(III)-oxo species are principally different from the rebound step considered in refs 20 and 23. The reasons for that will be discussed later in this section. The rebound stage in our scheme is a two-step process

including **3-oxoMin2→3-oxoMin3** and **3-oxoMin3→3-oxoTS→3-oxoMinP** transformations.

The rebound process starts with the recoordination of the PhC•(H)(OH) radical species from the copper center to the O1 atom. The total spin density in the PhC•(H)(OH) radical fragment of **3-oxoMin2** is 0.80, whereas after the recoordination of the radical fragment in **3-oxoMin3** it becomes one-half of the starting value (0.43). This is an indication of the significant transfer of the spin density to the copper complex in **3-oxoMin2→3-oxoMin3** transformation. The *s*(C1) values which are equal to 0.34 for **3-oxoMin2** and 0.17 for **3-oxoMin3** (see Table S8, Supporting Information) confirm this conclusion. The relative energy of thus formed **3-oxoMin3**, in which the PhCH(OH) moiety is coordinated to the complex with two hydrogen bonds H2···O1 (d = 1.530 Å) and H3···O1 (d = 2.380 Å), is 11.5 kcal/mol lower than for **3-oxoMin2**. The path **3-oxoMin2→3-oxoMin3** contains no stationary points, though in the energy scan profile along the O1−H2 coordinate given in Figure S1b (Supporting Information) a small peak (**3-oxoMid2**) of about 1 kcal/mol can be observed.

The second step of the rebound process is associated with H-atom transfer in **3-oxoMin3** (now it is the H2 atom) yielding **3-oxoMinP** in which the (biQ)Cu-fragment is coordinated to benzaldehyde and a water molecule, thus finishing the oxidation. This transformation gives an energy stabilization of 3.7 kcal/mol (Figure 7). The single found transition state **3-oxoTS** is associated with this transformation. It corresponds to an energy barrier of 0.8 kcal/mol (when E_e^r values are considered), whereas the analysis of E_0^r values does not confirm the presence of the activation barrier in this process (see Table S8, Supporting Information). **3-oxoTS** corresponds to equidistant H2 position between O1 (d = 1.215 Å) and O2 (d = 1.207 Å) atoms. The imaginary frequency of the H atom oscillations between two O atoms is 656i cm^{-1}, and it is close to the value obtained for **3-TS3** (898i cm^{-1}), which also corresponds to H-atom transfer between the two oxygen atoms (see Figure 2).

Now let us discuss the reasons for the difference in the rebound step observed for the triplet state in our computation and in the papers.[20,23,25] As it was demonstrated in refs 20, 23, and 25, the OH group transfer from the copper atom to the radical carbon center exhibits a very high activation barrier of 51.6,[20] 38.8,[23] and 37.3[25] kcal/mol (for the triplet state). According to atomic spectra data, the energy of Cu(I) in the $3d^9 4s^1$ triplet state is about 66 kcal/mol higher than that for the ground electronic state.[49] As follows from refs 20 and 23, the main reason for the high activation barrier for the OH group transfer is the involvement of the Cu(I) atom in the triplet state with an unstable $3d^9 4s^1$ electron configuration in the transition state.[20,23] In our opinion, this is also a crucial factor determining the absence of an OH-group transfer step in the mechanism considered above (Figure 7). The molecular structure of the system under consideration allows the performance of a rebound step in an alternative way, through almost barrierless **3-oxoMin2→3-oxoMin3** and **3-oxoMin3→3-oxoMinP** transformations (Figure 7), which do not involve the Cu−O bond breaking.

The stabilization energy of the preproduct **3-oxoMinP** relative to the **3-oxoReags** is 51 kcal/mol. This value is the maximum among all above considered reaction paths with the participation of the triplet complex (path A and path B, see Figures 1 and 2). It is comparable with the E_0^r obtained for **1-MinP** (−56.5 kcal/mol), corresponding to the oxidation of benzyl alcohol with the singlet (biQ)Cu(II)-superoxo complex (Figures 3 and 4). The strong coordination of benzaldehyde to the Cu center in **3-oxoMinP** originates from a lack of the other well-coordinated ligands (as in **3-MinP**). It results in significant shortening of the Cu···O2 distance in **3-oxoMinP** (d = 1.909 Å; compared with 2.202 Å, the value obtained for **3-MinP**) and consequent elongation of the carbonyl C1−O2 bond (d = 1.283 Å; compare with 1.246 Å, the value obtained for **3-MinP**). Consequently, the release of the benzaldehyde molecule should lead to strong destabilization of the system. For a reasonable estimation of relative energy values of the products formed in the oxidation process, the vacant coordination place in the Cu coordination environment can be occupied by the molecules of a solvent (e.g., CH_3CN). The thus calculated E_0^r for **3-oxoProds** is equal to −50.6 kcal/mol, a value close to the relative energy of **3-oxoMinP**. The obtained (biQ)Cu(I) complex, when reacting with dioxygen, can start a new catalytic cycle.

III.3.b. The Singlet State. Now let us consider the mechanism of benzyl alcohol oxidation with the (biQ)Cu(III)-oxo complex in a singlet state. The calculated energy profile is given in Figure 8; the relative energies, calculated atomic charges (q), and spin densities (s) of the species involved in the process are presented in Table S10 (Supporting Information). As follows from Figure 8, the reaction path consists of three minima and no transition states, and it substantially differs from the previously considered path with the participation of the triplet complex.

According to our computation data, the energy of the starting reagents in a singlet state (**1-oxoReags**) is 5.4 kcal/mol higher as compared to **3-oxoReags** (Figure 8). Almost the same values, 4.6[20] and 4.9[25] kcal/mol, were obtained in the literature. The coordination of benzyl alcohol to the copper atom in the (biQ)Cu(III)-oxo complex lowers the energy to 12.8 kcal/mol (Figure 8). This value is close to that obtained for the triplet system (13.9 kcal/mol; Figure 7) and is 4 kcal/mol higher than that obtained in ref 20 (ΔE_0^{r1} = 8.8 kcal/mol). Overestimated values of the coordination energy obtained for our system, as compared to the results of ref 20, are primarily attributed to the coordination of benzyl alcohol to the copper center, whereas in the paper[20] mentioned above, the hydrogen bonds in the reactant complex give the main contribution to the stabilization energy.

In the next reaction step, the benzylic H-atom abstraction already results in a barrierless 63.4 kcal/mol decrease in energy. This step does not lead to the formation of a product similar to the triplet **3-oxoMin2** embracing the PhC•(H)OH radical. Instead, it spontaneously goes ahead, and this radical abstracts the hydroxy group from the Cu center yielding the diol (Figure 8 and Figure S2, Supporting Information). In the energy scan for the

(49) Moore, C. E. *Atomic Energy Levels*: U.S. National Bureau of Standards: Washington, DC, 1949; circular 467.

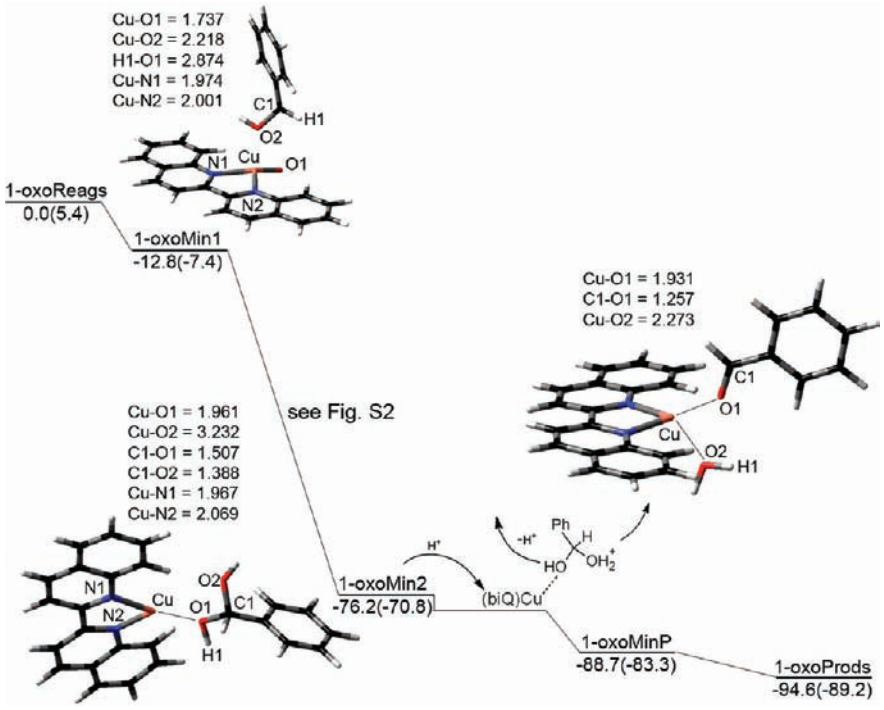

Figure 8. Potential energy profile (in kcal/mol) for benzyl alcohol oxidation with Cu(III)-oxo species (singlet electronic state). The specified energies correspond to $E_0^{\tau 1}$ and $E_0^{\tau 3}$ (in parentheses). All distances are given in Å.

O1−H1 distance parameter (Figure S2), two sections can be isolated: a flat plateau (up to 0.6) and an abrupt comedown (after 0.6). The plateau is responsible for the coordinative adjustment of the benzyl alcohol molecule for the further benzylic H-atom transfer to the O-atom of Cu(III)-oxo complex. The energy change in this location is small because it is not coupled with bond breaking or bond formation. After passing 0.6, significant changes in the **1-oxoMin1** molecular structure occur, associated with the C1−H1 bond breaking and O1−H1 bond formation, as well as with the formation of a new C1−O1 bond and simultaneous breaking of the Cu−O1 bond. These transformations lead to an energy stabilization of approximately 60 kcal/mol.

The mechanism considered for the singlet state has no principal differences from the mechanism suggested in refs 20, 23, and 25. The only exception concerns the **1-oxoMin1→1-oxoMin2** transformation, which is barrierless in our case and in the case of a large whole-enzyme model considered in ref 23, whereas for a small model,[20] two lower activation barriers were observed: 0.8 kcal/mol for the H-abstraction step and 6.5 kcal/mol for the rebound step.[20] Similar activation barriers for the H-abstraction step of $E_0^{\neq} = 1.8$ kcal/mol[25] and for the rebound step of $E_0^{\neq} = 5.4$ kcal/mol[25] were obtained in the PHM-catalyzed hydroxylation of peptidylglycine. The rebound step in our case also includes OH-radical transfer from the copper atom to the benzylic carbon center (Figure 8 and Figure S2, Supporting Information). However, it should be emphasized that the path considered here for the singlet state substantially differs from the mechanism proposed in the present paper for the triplet state and discussed above (Figure 7). As has been already mentioned, the main reason for this difference is an extremely unstable $3d^94s^1$ electron configuration of the triplet Cu(I). The $3d^{10}$ ground electron configuration inherent to the singlet Cu(I) is 66 kcal/mol[49] lower in energy than that of $3d^94s^1$. This provides the possibility of a barrierless rebound step including Cu−O bond breaking in the process presented in Figure 8.

Due to the geometric restrictions, the conversion of **1-oxoMin2** to **1-oxoMinP** is possible only in the case of the intermolecular transfer of a proton, which coordinates to the O2 atom (Figure 8). This is followed by the other proton expulsion (from the O1 atom) and a water molecule abstraction coupled to its coordination to the Cu center, yielding a preproduct (**1-oxoMinP**), which has an energy 12.5 kcal/mol lower than that for **1-oxoMin2**. The E_e^r and E_0^r energies of **1-oxoProds** were calculated with the molecule of acetonitrile as an additional ligand, for the same reasons, as in consideration of the triplet state of the oxo complex. For convenience, the complete comparison of two possible routes (for singlet and triplet states) will be given in section IV (Discussion).

IV. Discussion

It is interesting to perform a comparative analysis of all reaction paths presented above for the two most probable types of reactive species: (biQ)Cu(II)-superoxo and (biQ)Cu(III)-oxo complexes. We will start with the consideration of the (biQ)Cu(II)-superoxo reactant. For comparison, the zero energy level was selected respectively to **3-Reags** because the energy of the triplet η^2-(biQ)Cu(II)-superoxo complex (**3-η^2**) is the lowest (see Table 1). In further comparative considerations of (biQ)Cu(III)-oxo complexes with different multiplicities, the zero energy level corresponds to **3-oxoReags**.

IV.1. A Comparative Analysis of the Triplet and Singlet Paths: (biQ)Cu(II)-Superoxo Complex. The PBE/SBK-TZ exploration of two reaction paths (paths A and B) for

benzyl alcohol oxidation with a model (biQ)Cu(II)-superoxo complex performed for both the triplet and singlet states revealed that none of them is forbidden. Both investigated pathways are exothermic. The calculated $\Delta_r G^\circ_{298}$ values for paths A and B are equal because the starting reagents (**1-Reags** and **3-Reags**), as well as the products (**1-Prods** and **3-Prods**), are the same for both paths (Figures 1−4). The estimated $\Delta_r G^\circ_{298}$ value for the triplet state is equal to −28.4 kcal/mol, whereas for the singlet paths the value is substantially higher ($\Delta_r G^\circ_{298}$ = −44.9 kcal/mol respective to **1-Reags** and −41.0 kcal/mol respective to the **3-Reags**, Table 2).

The initial steps (up to **TS1**) for both pathways are the same. The estimation of activation barriers for all steps revealed that the highest value corresponds to the **Min1→TS1→Min2** process, thus indicating hydrogen atom abstraction to be a rate-determining step of both reaction pathways, as has been repeatedly mentioned earlier.

To choose the most probable reaction pathway, it is worth it to compare the complete energy profiles for both reaction paths. All investigated possibilities are summarized in Figure 9. The substantial difference in the behavior of the singlet and the triplet states of Cu(II)-superoxo species comes out in the vicinity of **Min2**. The energy of **1-Min2** in the singlet state is ∼36 kcal/mol lower as compared to that of the **3-Min2a** triplet state; hence, **TS1→Min2** passing should involve a spin-inversion electronic process in the vicinity of a crossing between the triplet and singlet potential energy surfaces. Spin−orbit coupling of the copper atom plays an important role in this process. It should be noted that spin inversion electronic processes are not so rare in transition-metal-mediated reactions.[38−42] The essential difference in energy of **3-Min2a** and **1-Min2** is attributed to their substantially different structure. **3-Min2a** possesses a radical character, whereas **1-Min2** is a closed−shell singlet species comprising benzaldehyde and hydrogen peroxide molecules.

If the reaction path *via* **1-Min2** is considered as the most probable one, it may have three possible continuations. Two of them are attributed to the singlet state (**1-Min2→1-TS2** and **1-Min2→1-MinP**). The third direction involves an additional spin inversion and leads to **3-MinP** yielding **3-Prods**. Analysis of the E_0^r values (Figures 1−4 and 9) allows concluding that the most probable route is the second direction: **1-Min2→1-MinP→1-Prods**. The realization of the **1-Min2→1-TS2** reaction path and its further continuation provides the same energy stabilization of the overall reaction. However, passing from **1-Min2** to **1-TS2** requires overcoming a considerable energy barrier (17.5 kcal/mol) comparable to the $E_0^{\neq}$ value for **3-Min1→3-TS1**. If it is yet realized, it is followed by the spin inversion yielding **3-Min3**. The continuation of this route involves the triplet species, but, as follows from Figure 9, the singlet potential energy surface lies very close to the triplet one, and in the vicinity of **TS-4**, one more spin inversion occurs (**3-Min4→1-TS4**). The benzaldehyde molecule's release from **1-MinP** gives the final products of the overall process **1-Prods** [(biQ)Cu(III)$(OH)_2$ and PhCHO] ($\Delta_r G^\circ_{298}$ = −41.0 kcal/mol, Table 2).

Thus, the most energetically favorable reaction path which specifies the sequence of the stationary points with minimal energy at each reaction step and involves several spin inversions is shown in Figure 9 with empty arrows. However, the final point of the reaction might also be a formation of **3-Prods** [(biQ)Cu(III)$(OH)_2$ and PhCHO] if the reaction passes through **3-MinP**. This reaction path includes only one spin inversion (in the **1-Min2→3-MinP** step) and is 13 kcal/mol less exothermic, but it is more simple.

Table 2. Changes in Standard Gibbs Energies[a] (in kcal/mol) for Reaction Paths Discussed in this Paper

	triplet species		singlet species	
	path A/B	oxo	path A/B	oxo
$\Delta_r G^\circ_{298}$	−28.4	−41.7	−44.9 (−41.0)	−87.3(−80.9)

[a] The values in parenthesis are calculated relatively to starting reagents in the triplet state.

IV.2. A Comparative Analysis of the Triplet and Singlet Paths: (biQ)Cu(III)-Oxo Complex. As mentioned above, in the course of alcohol oxidation with an initially formed Cu(II)-superoxo complex *via* paths A and B, the Cu(III)-oxo complex is formed, which can be involved in another catalytic cycle. The comparison of the energy profiles

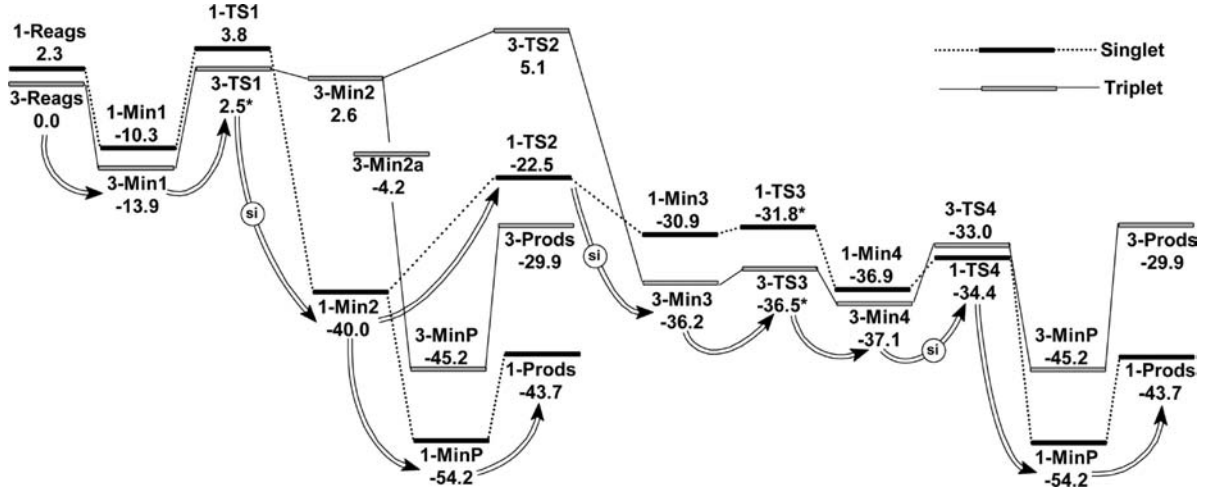

Figure 9. Summary of the DFT exploration of two reaction paths (path A and path B) for benzyl alcohol oxidation with the triplet and singlet (biQ)Cu(II)-superoxo complex.

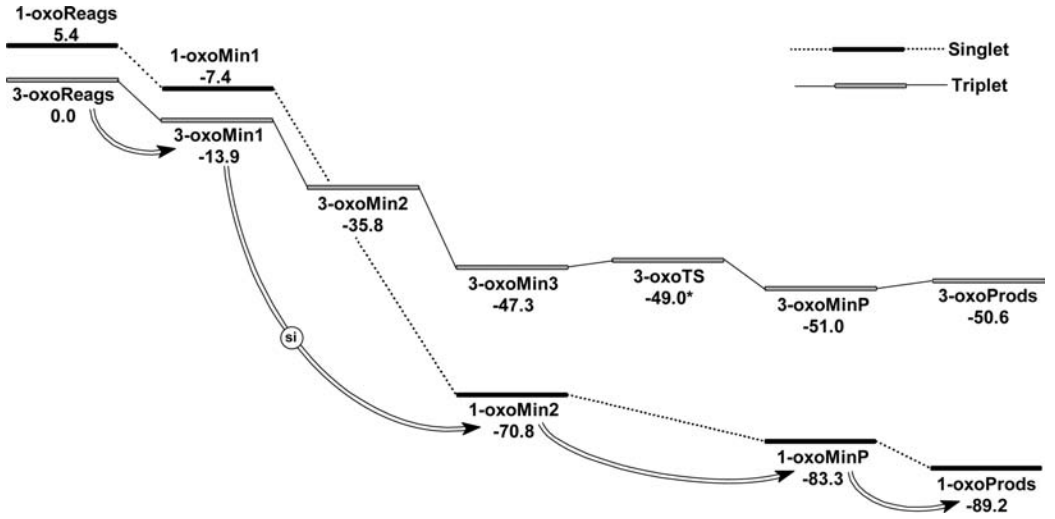

Figure 10. Summary of the DFT exploration of benzyl alcohol oxidation with the (biQ)Cu(III)-oxo complex, performed for both the triplet and singlet states.

Scheme 6

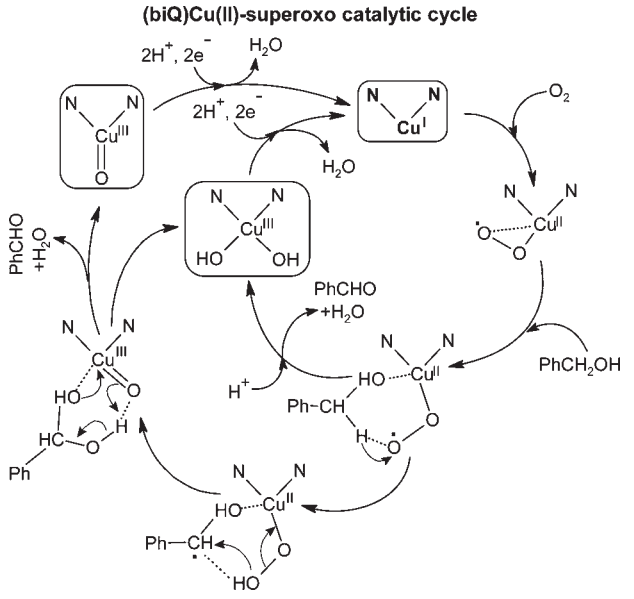

Scheme 7

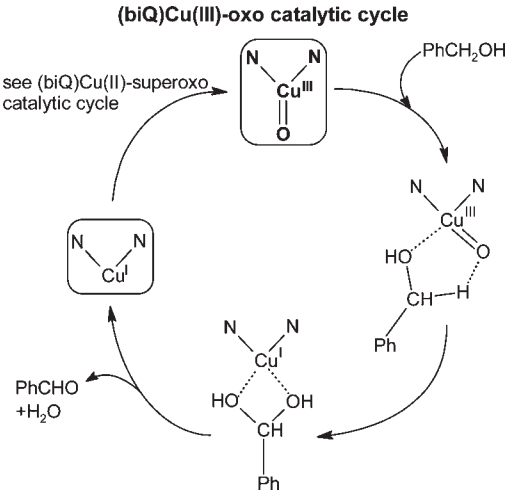

obtained for the oxidation of benzyl alcohol with the (biQ)Cu(III)-oxo complex in the singlet and triplet states is given in Figure 10. In the beginning of the process, the energy gap between the triplet and singlet surfaces is small (5−6 kcal/mol), and the continuation of the reaction provides significant stabilization of the singlet intermediates, thus changing the relative order of the spin states. The **3-oxoMin1→1-oxoMin2** conversion involves the single spin inversion in the whole reaction path. It should be mentioned that the spin inversion was also disclosed[20,23] in the oxidation of dopamine with the Cu(III)-oxo complex. The process follows the singlet path and yields **1-oxoProds** [(biQ)Cu(I)(H_2O) and PhCHO] ($\Delta_r G^\circ_{298}$ = −80.9 kcal/mol, Table 2). This route is barrierless and the most exothermic among all the processes discussed above and seems to be the most favorable. It is marked in Figure 10 with empty arrows. In the papers mentioned above, the $\Delta E_0^{\ddagger}$ values are substantially lower (as compared to our data): −46.6[20] and −60.6.[23]

Thus, DFT calculations revealed that the (biQ)Cu(III)-oxo complex should be a more active oxidant in benzyl alcohol conversion to benzaldehyde, as compared to the (biQ)Cu(II)-superoxo system. Our results are in good agreement with the data of refs 20 and 23. The authors[20,23] came to the same conclusion after DFT evaluation of the dopamine hydroxylation with the Cu(III)-oxo and Cu(II)-superoxo systems.

V. Conclusion

Analysis of the summarizing Figures 9 and 10, as well as referring to the experimental details of electrocatalytic aerobic oxidation of alcohols in the presence of (biQ)Cu(I) complexes discussed in refs 14 and 15, allows for the following conclusion.

The reaction starts with the oxidation of alcohol with the (biQ)Cu(II)-superoxo complex because it is initially formed in the interaction of starting (biQ)Cu(I) species with a molecular dioxygen. The oxidation can follow path A or path B, and both reaction pathways are reasonable. Indeed, the existence of parallel pathways cannot be ruled out. But path A is less complicated, and the entropy factor should facilitate

this route. The products comprise benzaldehyde and the (biQ)Cu(III)$(OH)_2$ complex, with intermediate formation of (biQ)Cu(III)-oxo species in **Min3**. (biQ)Cu(III)$(OH)_2$ and (biQ)Cu(III)═O complexes can be further reduced at the electrode at the potential applied (−0.55 V vs Ag/AgCl/KCl) in the presence of protons, thus finishing the catalytic cycle and restoring the catalyst.

The other probable opportunity is further involvement of a previously formed (biQ)Cu(III)-oxo species in the catalytic oxidation of the benzyl alcohol. As our DFT exploration revealed, this process is barrierless and much more exothermic and, consequently, should be rather fast. It also includes the α-H-atom abstraction step and yields benzaldehyde, a water molecule, and an initial (biQ)Cu(I) complex.

The important experimental observation which agrees with the computation data is that the reaction needs an external source of protons. According to our experimental data,[15] the reaction is very sensitive to the presence of water. It does not occur in thoroughly dried acetonitrile and when specially dried air is bubbled through the cell. When a certain amount of water is added (approximately 5%), the current increases dramatically, thus indicating the beginning of the catalytic reaction. A comparative computational analysis of a variety of possible reaction paths (see Figure 9 and Discussion) revealed that after **1-Min2** two alternative continuations of the process are possible, one of which corresponds to path A (singlet) and the other to path B (singlet). In the first case, the reaction is barrierless in the presence of a source of protons. In the second case, it is necessary to overcome a high energy barrier (17.5 kcal/mol) corresponding to the **1-Min2**→**1-TS2**→**3-Min3** transformation. Thus, formally the reaction can proceed even in the absence of water, but it might be expected to be very slow and less probable. Additionally, water molecules play a role of a source of protons which are necessary for a spontaneous cleavage of the peroxide bond yielding the Cu(III)-oxo complex coordinated to biQ and benzaldehyde (see section III.2.c). Therefore, the addition of water or another source of protons should facilitate the overall oxidation process.

The experimental reaction is an electrocatalytic process occurring at a potential of Cu(II)/Cu(I) transfer (−0.55 V vs Ag/AgCl/KCl); it does not proceed when the potential is switched off. Additional electrons are also necessary to restore the catalyst in the proposed mechanism. This fact can be considered as an additional argument in favor of our mechanism.

Thus, the overall catalytic process can be considered as a combination of two interdependent catalytic cycles. The starting catalytic cycle, in which the Cu-superoxo complex performs the process (Scheme 6), can be coupled to the second cycle (Scheme 7), which is governed by the Cu-oxo complex formed in the first cycle. The first cycle presented in Scheme 6 is a simplified version of paths A and B.

Finally, it should be emphasized that the conclusions above are based on thermodynamic consideration and an evaluation of activation barriers. In real systems, solvation and diffusion effects usually play an essential role and often import corrections in the reaction course. Nevertheless, our computations on model systems may be helpful in the interpretation of the experimental results.

Acknowledgment. The work was financially supported by the Russian Foundation for Basic Research (project N 08-03-00142). The Joint Supercomputer Center of Russian Academy of Science (JSCC, Moscow) is acknowledged for the computing facilities.

Note Added after ASAP Publication. This paper was published on the Web on February 25, 2010, with the wrong page ranges in ref 17. The corrected version was reposted on March 2, 2010.

Supporting Information Available: Additional figures; cartesian coordinates for geometry optimized structures (about 50 species); tables presenting atomic charges, spin populations, and absolute and relative electronic energies of the described species. This material is available free of charge *via* the Internet at http://pubs.acs.org.